

# Quantum Deep Learning

Nathan Wiebe, Ashish Kapoor, and Krysta M. Svore  
*Microsoft Research, Redmond, WA (USA)*

In recent years, deep learning has had a profound impact on machine learning and artificial intelligence. Here we investigate if quantum algorithms for deep learning lead to an advantage over existing classical deep learning algorithms. We develop two quantum machine learning algorithms that reduce the time required to train a deep Boltzmann machine and allow richer classes of models, namely multi-layer, fully connected networks, to be efficiently trained without the use of contrastive divergence or similar approximations. Our algorithms may be used to efficiently train either full or restricted Boltzmann machines. By using quantum state preparation methods, we avoid the use of contrastive divergence approximation and obtain improved maximization of the underlying objective function.

## I. INTRODUCTION

Deep learning is a recent technique for machine learning that has substantially impacted the way in which classification, inference, and artificial intelligence (AI) tasks are modeled [1–4]. Deep learning emerged based on the premise that to perform sophisticated AI tasks, in areas such as speech and vision, it may be necessary to allow a machine to learn a model that contains several layers of abstractions of the raw input data. For example, an inference model trained to detect a car might first accept a raw image, in pixels, as input. In a subsequent layer, it may abstract the data into simple shapes. In the next layer, the elementary shapes may be abstracted further into aggregate forms, such as bumpers or wheels. At even higher layers, the shapes may be tagged with words like “tire” or “hood”. Deep networks, therefore, have been developed to automatically learn a complex, nested representation of raw data, similar to layers of neuron processing in our brain, where ideally the learned hierarchy of concepts is (humanly) understandable. In general, deep networks may contain many levels of abstraction encoded into a highly connected, complex graphical network; training such graphical networks falls under the umbrella of deep learning.

One class of deep networks are Boltzmann machines, which consist of a complete graph with a weighted edge between any two nodes in the graph. These nodes, also called units, encode features and concepts automatically inferred from the raw data. The edges describe the ways in which the units can communicate with each other. Exact training Boltzmann machines is intractable since calculation of the gradient of the objective function requires computation of the so-called partition function  $Z$ , which is known to be  $\#P$ -hard to compute and cannot in general be efficiently approximated within a specified multiplicative error (unless  $RP=NP$ ). Therefore, modulo reasonable complexity theoretic assumptions, neither a quantum nor a classical computer should be able to directly compute the probability of a given model configuration and in turn compute the log-likelihood of the Boltzmann machine yielding the particular configuration of the units. In practice, however, approximations of the gradient of the log-likelihood are based on contrastive divergence and in some cases mean-field assumptions [3, 5–8]. Unfortunately, these approaches do not provide the gradient of any true objective function [9]. Therefore, learning with methods such as contrastive divergence can lead to suboptimal points in the space of the objective function [10–12], and in fact is not guaranteed to converge in the presence of certain regularization functions [9]. In addition, contrastive divergence cannot be used to train a full Boltzmann machine (BM). To circumvent the challenge of training BMs, deep restricted Boltzmann machines (dRBM) in which each layer of hidden units is restricted to connections to units only in adjacent layers are used. Training dRBMs requires greedy layer-by-layer training, which is costly when the number of layers is large, but at least allows the use of the contrastive divergence approximation to efficiently train each layer.

In this paper, we examine if alternate strategies exist, namely quantum strategies, that enable efficient training of both dRBMs and full BMs without the use of gradient approximations like contrastive divergence. Recent work has shown that quantum algorithms can offer speedups relative to their classical analogs for problems such as regression [13, 14], classification and clustering [15–19], and inference [20]. Other work [21] suggests that quantum computers may be able to find superior solutions to classification or optimization problems than those found using classical methods. We show that quantum computing has the potential to not only accelerate the training process for Boltzmann machines relative to state-of-the-art methods but to also increase the quality of the models learned. Our quantum algorithms offer more efficient training of both dRBMs and BMs than existing classical algorithms and use few additional quantum resources. Moreover, our quantum algorithms offer improved maximization of the objective function, leading to more accurate models. In summary, we find that quantum computers indeed appear to be able to perform an important machine learning task that is not known to be classically tractable.

The paper proceeds as follows. We provide an introduction to Boltzmann machines in [Section II](#) and a review of quantum computing in [Section III](#). [Section IV](#) gives our algorithm for preparing the coherent quantum Gibbs and

mean-field states needed to train our model. We provide in [Section V](#) a quantum algorithm for training a deep Boltzmann machine that is based on sampling and give a similar algorithm based on quantum amplitude estimation in [Section VI](#). We then present numerical experiments on small Boltzmann machines in [Section VII](#) before concluding.

## II. BOLTZMANN MACHINES

The Boltzmann machine is a powerful machine learning model in which the problem of training a system to classify a set of input training vectors, or equivalently generate samples from an input distribution, is reduced to the problem of energy minimization of an Ising spin system. The Boltzmann machine is a graphical model where each node, or unit, represents a feature of the data (or inferred feature of the data) and each edge in the graph describes the interactions that the Boltzmann machine uses to either classify the input data or generate a training example. The Boltzmann machine consists of units that are split into two categories: (a) visible units and (b) hidden units (see [Figure 1](#)). The visible units encode the input and output of the model. For example, if the model is used for classification then the visible units may encode the raw training data along with a corresponding label. The hidden units model complex correlations between the visible units. Learning these correlations enables the model either to assign an appropriate label to a given training vector or to generate a sample of the type of data the model is trained to output. We use the variables  $v$  and  $h$  to denote visible and hidden units, respectively. For simplicity, we assume that the hidden and visible units are binary.

More formally, a Boltzmann machine models the probability of a given configuration of hidden and visible units based on the Gibbs distribution (with inverse temperature 1):

$$P(v, h) = e^{-E(v, h)} / Z, \quad (1)$$

where  $Z$  is a normalizing factor known as the *partition function* and the energy  $E(v, h)$  of a given configuration  $(v, h)$  of hidden and visible units is given for the full Boltzmann machine by

$$E(v, h) = - \sum_i v_i b_i - \sum_j h_j d_j - \sum_{i,j} w_{i,j}^{vh} v_i h_j - \sum_{i,j} w_{i,j}^v v_i v_j - \sum_{i,j} w_{i,j}^h h_i h_j. \quad (2)$$

Here the vectors  $b$  and  $d$  are *biases* that provide an energy penalty for a unit taking the value of 1 and  $w_{i,j}^{v,h}$ ,  $w_{i,j}^v$  and  $w_{i,j}^h$  are *weights* which assigns an energy penalty if the hidden and visible units both take value 1. We will often refer to all three of these types of weights collectively and group them together as a single vector  $w = [w^{vh}, w^v, w^h]$ .

There are several important cases of Boltzmann machines that we consider in this paper. The case of the restricted Boltzmann machine (RBM) arises when direct couplings between visible and visible or hidden and hidden units are forbidden (i.e.  $w^h = w^v = 0$ ). The deep restricted Boltzmann machine (dRBM) is formed out of several layers of RBM models and is constrained such that  $w^v = 0$  and  $w_{i,j}^h = 0$  unless  $h_i$  and  $h_j$  are on adjacent layers of the dRBM (see [Figure 1](#)).

Training a Boltzmann machine reduces to estimating the biases and weights that maximize the log-likelihood of the training data. Often an  $L2$ -regularization term is added in order to prevent overfitting, resulting in the following form of the objective function:

$$O_{\text{ML}} := \frac{1}{N_{\text{train}}} \sum_{v \in x_{\text{train}}} \log \left( \sum_h P(v, h) \right) - \frac{\lambda}{2} w^T w, \quad (3)$$

where  $\lambda$  represents the regularization term and  $N_{\text{train}}$  is the number of training examples. We refer to this objective function as the maximum-likelihood objective (ML-objective). Gradient ascent provides a means to find a locally

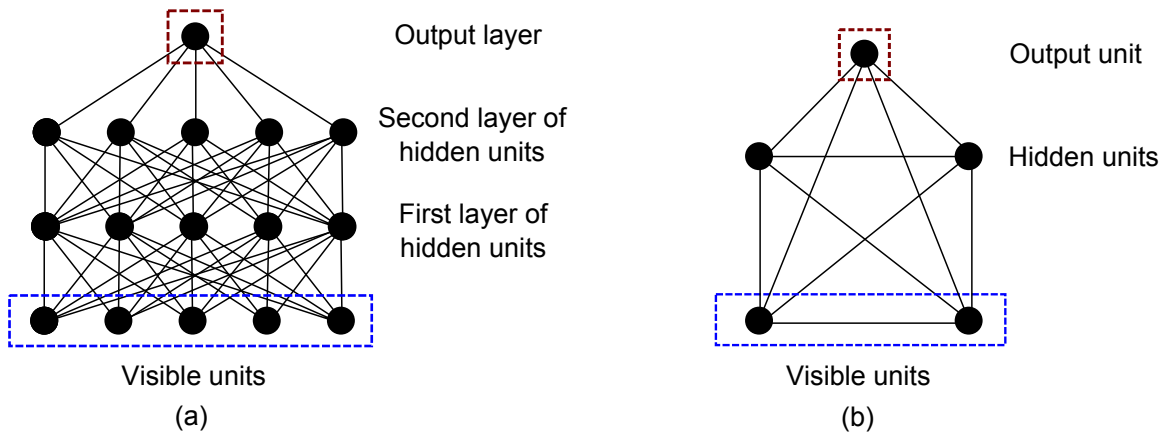


FIG. 1: A graphical representation of two types of Boltzmann machines. (a) A 4-layer dRBM where each black circle represents a hidden or visible unit and each edge represents a non-zero weight for the corresponding interaction. The output layer is often treated as a visible layer to provide a classification for data input into the visible units at the bottom of the graph. (b) An example of a 5-unit full Boltzmann machine. In this example the notion of hidden and visible units occupying distinct layers no longer holds because of direct connections between units of the same type.

optimal value of the ML-objective function. The gradients of the ML-objective for the BM are:

$$\begin{aligned}
 \frac{\partial O_{\text{ML}}}{\partial w_{i,j}^{v,h}} &= \langle v_i h_j \rangle_{\text{data}} - \langle v_i h_j \rangle_{\text{model}} - \lambda w_{i,j}^{v,h}. \\
 \frac{\partial O_{\text{ML}}}{\partial w_{i,j}^v} &= \langle v_i v_j \rangle_{\text{data}} - \langle v_i v_j \rangle_{\text{model}} - \lambda w_{i,j}^v. \\
 \frac{\partial O_{\text{ML}}}{\partial w_{i,j}^h} &= \langle h_i h_j \rangle_{\text{data}} - \langle h_i h_j \rangle_{\text{model}} - \lambda w_{i,j}^h. \\
 \frac{\partial O_{\text{ML}}}{\partial b_i} &= \langle v_i \rangle_{\text{data}} - \langle v_i \rangle_{\text{model}}. \\
 \frac{\partial O_{\text{ML}}}{\partial d_j} &= \langle h_j \rangle_{\text{data}} - \langle h_j \rangle_{\text{model}}.
 \end{aligned} \tag{4}$$

To clarify, the above expectation values for a quantity  $f(v, h)$  are given by

$$\langle f \rangle_{\text{data}} = \frac{1}{N_{\text{train}}} \sum_{x \in x_{\text{train}}} \sum_h \frac{f(x, h) e^{-E(x, h)}}{Z_x}, \tag{5}$$

where  $Z_x = \sum_h e^{-E(x, h)}$ , and

$$\langle f \rangle_{\text{model}} = \sum_{v, h} \frac{f(v, h) e^{-E(v, h)}}{Z}, \tag{6}$$

where  $Z = \sum_{v, h} e^{-E(v, h)}$ .

As stated earlier, it is non-trivial to compute these gradients: the value of the partition function  $Z$  is #P-hard to compute and cannot in general be efficiently approximated within a specified multiplicative error (unless RP=NP). This is what motivates approximations to the gradient, such as the contrastive divergence approximation [5]. In the remaining sections, we describe our quantum approach which allows us to compute these gradients by sampling.

### III. INTRODUCTION TO QUANTUM COMPUTING

In quantum information processing, information is stored in a quantum bit, or *qubit*, which is analogous to a classical bit. Whereas a classical bit has a state value  $s \in \{0, 1\}$ , a qubit state, denoted as  $|\psi\rangle$ , is actually a linear *superposition*

of states:

$$|\psi\rangle = \alpha|0\rangle + \beta|1\rangle, \quad (7)$$

where the  $\{0, 1\}$  basis state vectors are represented in Dirac notation (ket vectors) as  $|0\rangle = [1 \ 0]^T$ , and  $|1\rangle = [0 \ 1]^T$ , respectively. The *amplitudes*  $\alpha$  and  $\beta$  are complex numbers that satisfy the normalization condition:  $|\alpha|^2 + |\beta|^2 = 1$ . Upon *measurement* of the quantum state  $|\psi\rangle$ , either state  $|0\rangle$  or  $|1\rangle$  is observed with probability  $|\alpha|^2$  or  $|\beta|^2$ , respectively. Note that a  $n$ -qubit quantum state is a  $2^n \times 1$ -dimensional state vector, where each entry represents the amplitude of the corresponding basis state. Therefore,  $n$  qubits live in a  $2^n$ -dimensional Hilbert space, and we can represent a superposition over  $2^n$  states as:

$$|\psi\rangle = \sum_{i=0}^{2^n-1} \alpha_i |i\rangle, \quad (8)$$

where  $\alpha_i$  are complex amplitudes that satisfy the condition  $\sum_i |\alpha_i|^2 = 1$ , and  $i$  is the binary representation of integer  $i$ . Note, for example, that the state  $|0000\rangle$  is equivalent to writing the tensor product of the four states:  $|0\rangle \otimes |0\rangle \otimes |0\rangle \otimes |0\rangle = |0\rangle^{\otimes 4} = [1 \ 0 \ 0 \ 0 \ 0 \ 0 \ 0 \ 0]^T$ . A quantum state containing one or more qubits, such as the state  $|0000\rangle$ , may be called a *quantum register*. The ability to represent a superposition over exponentially many states with only a linear number of qubits is one of the essential ingredients of a quantum algorithm — an innate massive parallelism.

A quantum computation proceeds through a *unitary* evolution of a quantum state; in turn, quantum operations are necessarily *reversible*. We refer to quantum unitary operations as *quantum gates*. Note that measurement is not reversible; it collapses the quantum state to the observed value, thereby erasing the knowledge of the amplitudes  $\alpha$  and  $\beta$ .

An  $n$ -qubit quantum gate is a  $2^n \times 2^n$  unitary matrix acting on an  $n$ -qubit quantum state. For example, the *Hadamard* gate maps  $|0\rangle \rightarrow \frac{1}{\sqrt{2}}(|0\rangle + |1\rangle)$ , and  $|1\rangle \rightarrow \frac{1}{\sqrt{2}}(|0\rangle - |1\rangle)$ . An *X* gate, similar to a classical NOT gate, maps  $|0\rangle \rightarrow |1\rangle$ , and  $|1\rangle \rightarrow |0\rangle$ . The identity gate is represented by  $I$ . The two-qubit *controlled-NOT* gate, denoted  $CX$ , maps  $|x, y\rangle \rightarrow |x, x \oplus y\rangle$ . It is convenient to include an additional gate,  $T$ , which is known as a  $\pi/8$ -gate, to make the above quantum gate set *universal*, meaning any quantum algorithm can be approximated to arbitrary precision as a quantum circuit over gates drawn from this set. The corresponding unitary matrices are given by:

$$H = \frac{1}{\sqrt{2}} \begin{bmatrix} 1 & 1 \\ 1 & -1 \end{bmatrix}, X = \begin{bmatrix} 0 & 1 \\ 1 & 0 \end{bmatrix}, I = \begin{bmatrix} 1 & 0 \\ 0 & 1 \end{bmatrix}, CX = \begin{bmatrix} 1 & 0 & 0 & 0 \\ 0 & 1 & 0 & 0 \\ 0 & 0 & 0 & 1 \\ 0 & 0 & 1 & 0 \end{bmatrix}, T = \begin{bmatrix} 1 & 0 \\ 0 & e^{i\pi/4} \end{bmatrix}. \quad (9)$$

An alternative universal gate set consists of the above gates and a replacement of  $T$  with a so-called *Toffoli* gate. The three-qubit Toffoli gate is a controlled-controlled-NOT gate, denoted  $CCX$ , and maps  $|x, y, z\rangle \rightarrow |x, y, (x \wedge y) \oplus z\rangle$ . It can be equivalently implemented using gates from the above-listed universal set [22].

Single-qubit rotations are an important operation for quantum computation. The single-qubit rotation  $R_y(2\theta)$ , under the isomorphism between  $SO(3)$  and  $SU(2)$ , corresponds to a rotation of the state vector about the  $y$ -axis by an angle  $2\theta$ , where the states  $|0\rangle$  and  $|1\rangle$  are computational basis states. The gate is defined below:

$$R_y(2\theta) = \begin{bmatrix} \cos(\theta) & -\sin(\theta) \\ \sin(\theta) & \cos(\theta) \end{bmatrix}. \quad (10)$$

Unlike the previous gates, arbitrary single-qubit rotations are not discrete. They can, however, be approximated to within arbitrarily small precision using a sequence of fundamental (discrete) gates drawn from, for example, the set  $\{H, T\}$  [23–25].

#### IV. QUANTUM ALGORITHM FOR STATE PREPARATION

We begin by showing how quantum computers can draw unbiased samples from the Gibbs distribution, thereby allowing the probabilities  $P(v, h)$  to be computed by sampling (or by quantum sampling). The idea behind our approach is to prepare a quantum distribution that approximates the ideal probability distribution over the model or data. This approximate distribution is then refined using rejection sampling into a quantum distribution that is, to within numerical error, the target probability distribution [26]. If we begin with a uniform prior over the amplitudes

of the Gibbs state, then preparing the state via quantum rejection sampling is likely to be inefficient. This is because the success probability depends on the ratio of the partition functions of the initial state and the Gibbs state [27], which in practice is exponentially small for machine learning problems. Instead, our algorithm uses a mean-field approximation, rather than a uniform prior, over the joint probabilities in the Gibbs state. We show numerically that this extra information can be used to boost the probability of success to acceptable levels. The required expectation values can then be found by sampling from the quantum distribution. We show that the number of samples needed to achieve a fixed sampling error can be quadratically reduced by using a quantum algorithm known as amplitude estimation.

We first discuss the process by which the initial quantum distribution is refined into a quantum coherent Gibbs state (often called a coherent thermal state or CTS). We then discuss how mean-field theory, or generalizations thereof, can be used to provide suitable initial states for the quantum computer to refine into the CTS. We assume in the following that all units in the Boltzmann machine are binary valued. Other valued units, such as Gaussian units, can be approximated within this framework by forming a single unit out of a string of several qubits.

First, let us define the mean-field approximation to the joint probability distribution to be  $Q(v, h)$ . For more details on the mean-field approximation, see [Appendix A](#). We also use the mean-field distribution to compute a variational approximation to the partition functions needed for our algorithm. These approximations can be efficiently calculated (because the probability distribution factorizes) and are defined below.

**Definition 1.** Let  $Q$  be the mean-field approximation to the Gibbs distribution  $P$  (which is given in (1)) then

$$Z_{\text{MF}} := \sum_{v, h} Q(v, h) \log \left( \frac{e^{-E(v, h)}}{Q(v, h)} \right).$$

Furthermore for any  $x \in x_{\text{train}}$  let  $Q_x$  be the mean-field approximation to the Gibbs distribution found for a Boltzmann machine with the visible units clamped to  $x$ , then

$$Z_{x, \text{MF}} := \sum_h Q_x(x, h) \log \left( \frac{e^{-E(x, h)}}{Q_x(x, h)} \right).$$

In order to use our quantum algorithm to prepare  $P$  from  $Q$  we need to know an upper bound,  $\kappa$ , on the ratio of the approximation  $P(v, h) \approx e^{-E(v, h)}/Z_{\text{MF}}$  to  $Q(v, h)$ . We formally define this below.

**Definition 2.** Let  $\kappa > 0$  be a constant that is promised to satisfy for all visible and hidden configurations  $(v, h)$

$$\frac{e^{-E(v, h)}}{Z_{\text{MF}}} \leq \kappa Q(v, h), \quad (11)$$

where  $Z_{\text{MF}}$  is the approximation to the partition function given in [Definition 1](#).

**Lemma 1.** Let  $Q(v, h)$  be the mean-field probability distribution for a Boltzmann machine, then for all configurations of hidden and visible units we have

$$P(v, h) \leq \frac{e^{-E(v, h)}}{Z_{\text{MF}}} \leq \kappa Q(v, h).$$

*Proof.* The mean-field approximation can also be used to provide a lower bound for the log-partition function. For example, Jensen's inequality shows that

$$\begin{aligned} \log(Z) &= \log \left( \sum_{v, h} \frac{Q(v, h) e^{-E(v, h)}}{Q(v, h)} \right), \\ &\geq \sum_{v, h} Q(v, h) \log \left( \frac{e^{-E(v, h)}}{Q(v, h)} \right) = \log(Z_{\text{MF}}). \end{aligned} \quad (12)$$

This shows that  $Z_{\text{MF}} \leq Z$  and hence

$$P(v, h) \leq e^{-E(v, h)}/Z_{\text{MF}}, \quad (13)$$

where  $Z_{\text{MF}}$  is the approximation to  $Z$  that arises from using the mean-field distribution. The result then follows from (13) and [Definition 2](#).  $\square$

The result of [Lemma 1](#) allows us to prove the following lemma, which gives the success probability for preparing the Gibbs state from the mean-field state.

**Lemma 2.** *A coherent analog of the Gibbs state for a Boltzmann machine can be prepared with a probability of success of  $\frac{Z}{\kappa Z_{\text{MF}}}$ . Similarly, the Gibbs state corresponding to the visible units being clamped to a configuration  $x$  can be prepared with success probability  $\frac{Z_x}{\kappa_x Z_{x,\text{MF}}}$ .*

*Proof.* The first step in the algorithm is to compute the mean-field parameters  $\mu_i$  and  $\nu_j$  using [\(A3\)](#). These parameters uniquely specify the mean-field distribution  $Q$ . Next the mean-field parameters are used to approximate the partition functions  $Z$  and  $Z_x$ . These mean-field parameters are then used to prepare a coherent analog of  $Q(v, h)$ , denoted as  $|\psi_{\text{MF}}\rangle$ , by performing a series of single-qubit rotations:

$$|\psi_{\text{MF}}\rangle := \prod_i R_y(2 \arcsin(\sqrt{\mu_i})) |0\rangle \prod_j R_y(2 \arcsin(\sqrt{\nu_j})) |0\rangle = \sum_{v,h} \sqrt{Q(v, h)} |v\rangle |h\rangle. \quad (14)$$

The remaining steps use rejection sampling to refine this crude approximation to  $\sum_{v,h} \sqrt{P(v, h)} |v\rangle |h\rangle$ .

For compactness we define

$$\mathcal{P}(v, h) := \frac{e^{-E(v, h)}}{\kappa Z_{\text{MF}} Q(v, h)}. \quad (15)$$

Note that this quantity can be computed efficiently from the mean-field parameters and so an efficient quantum algorithm (quantum circuit) also exists to compute  $\mathcal{P}(v, h)$ . [Lemma 1](#) guarantees that  $0 \leq \mathcal{P}(v, h) \leq 1$ .

Since quantum operations are linear, if we apply the algorithm to a state  $\sum_v \sum_h \sqrt{Q(v, h)} |v\rangle |h\rangle |0\rangle$  we obtain  $\sum_v \sum_h \sqrt{Q(v, h)} |v\rangle |h\rangle |\mathcal{P}(v, h)\rangle$ . We then add an additional quantum bit, called an ancilla qubit, and perform a controlled rotation of the form  $R_y(2 \sin^{-1}(\mathcal{P}(v, h)))$  on this qubit to enact the following transformation:

$$\sum_{v,h} \sqrt{Q(v, h)} |v\rangle |h\rangle |\mathcal{P}(v, h)\rangle |0\rangle \mapsto \sum_{v,h} \sqrt{Q(v, h)} |v\rangle |h\rangle |\mathcal{P}(v, h)\rangle \left( \sqrt{1 - \mathcal{P}(v, h)} |0\rangle + \sqrt{\mathcal{P}(v, h)} |1\rangle \right). \quad (16)$$

The quantum register that contains the qubit string  $\mathcal{P}(v, h)$  is then reverted to the  $|0\rangle$  state by applying the same operations used to prepare  $\mathcal{P}(v, h)$  in reverse. This process is possible because all quantum operations, save measurement, are reversible. Since  $\mathcal{P}(v, h) \in [0, 1]$ , then [\(16\)](#) is a properly normalized quantum state and in turn its square is a valid probability distribution.

If the rightmost quantum bit in [\(16\)](#) is measured and a result of 1 is obtained (recall that projective measurements always result in a unit vector) then the remainder of the state will be proportional to

$$\sum_{v,h} \sqrt{Q(v, h) \mathcal{P}(v, h)} = \sqrt{\frac{Z}{\kappa Z_{\text{MF}}}} \sum_{v,h} \sqrt{\frac{e^{-E(v, h)}}{Z}} |v\rangle |h\rangle = \sqrt{\frac{Z}{\kappa Z_{\text{MF}}}} \sum_{v,h} \sqrt{P(v, h)} |v\rangle |h\rangle, \quad (17)$$

which is the desired state up to a normalizing factor. The probability of measuring 1 is the square of this constant of proportionality

$$P(1|\kappa, Z_{\text{MF}}) = \frac{Z}{\kappa Z_{\text{MF}}}. \quad (18)$$

Note that this is a valid probability because  $Z \geq Z_{\text{MF}}$  and  $\kappa \geq 1$ .

Preparing a quantum state that can be used to estimate the expectation values over the data requires a slight modification to this algorithm. First, for each  $x \in x_{\text{train}}$  needed for the expectation values, we replace  $Q(v, h)$  with the constrained mean-field distribution  $Q_x(x, h)$ . Then using this data the quantum state

$$\sum_h \sqrt{Q_x(x, h)} |x\rangle |h\rangle, \quad (19)$$

can be prepared. We then follow the exact same protocol using  $Q_x$  in place of  $Q$ ,  $Z_x$  in place of  $Z$ , and  $Z_{x,\text{MF}}$  in place of  $Z_{\text{MF}}$ . The success probability of this algorithm is

$$P(1|\kappa, Z_{x,\text{MF}}) = \frac{Z_x}{\kappa_x Z_{x,\text{MF}}}, \quad (20)$$

where  $\kappa_x$  is the value of  $\kappa$  that corresponds to the case where the visible units are clamped to  $x$ .  $\square$

---

**Algorithm 1** Quantum algorithm for generating states that can be measured to estimate the expectation values over the model.

---

**Input:** Model weights  $w$ , visible biases  $b$ , hidden biases  $d$ , edge set  $E$  and  $\kappa$ .

**Output:** Quantum state that can be measured to obtain the correct Gibbs state for a (deep) Boltzmann machine.

---

**function** QGENMODELSTATE( $w, b, d, E, \kappa$ )

  Compute vectors of mean-field parameters  $\mu$  and  $\nu$  from  $w, b$  and  $d$ .

  Compute the mean-field partition function  $Z_{\text{MF}}$ .

  Prepare state  $\sum_{v,h} \sqrt{Q(v,h)} |v\rangle |h\rangle := \left( \prod_{i=1}^{n_v} e^{-i\sqrt{\mu_i} Y} |0\rangle \right) \left( \prod_{j=1}^{n_h} e^{-i\sqrt{\nu_j} Y} |0\rangle \right)$

  Add qubit register to store energy values and initialize to zero:  $\sum_{v,h} \sqrt{Q(v,h)} |v\rangle |h\rangle \rightarrow \sum_{v,h} \sqrt{Q(v,h)} |v\rangle |h\rangle |0\rangle$

**for**  $i = 1 : n_v$  **do**

$\sum_{v,h} \sqrt{Q(v,h)} |v\rangle |h\rangle |E(v,h)\rangle \rightarrow \sum_{v,h} \sqrt{Q(v,h)} |v\rangle |h\rangle |E(v,h) + v_i b_i + \ln(\mu_i^{v_i} (1 - \mu_i)^{1-v_i})\rangle$ .

    ▷ Here an energy penalty is included to handle the bias and the visible units contribution to  $Q(v,h)^{-1}$ .

**end for**

**for**  $j = 1 : n_h$  **do**

$\sum_{v,h} \sqrt{Q(v,h)} |v\rangle |h\rangle |E(v,h)\rangle \rightarrow \sum_{v,h} \sqrt{Q(v,h)} |v\rangle |h\rangle |E(v,h) + h_j d_j + \ln(\nu_j^{h_j} (1 - \nu_j)^{1-h_j})\rangle$ .

**end for**

**for**  $(i,j) \in E$  **do**

$\sum_{v,h} \sqrt{Q(v,h)} |v\rangle |h\rangle |E(v,h)\rangle \rightarrow \sum_{v,h} \sqrt{Q(v,h)} |v\rangle |h\rangle |E(v,h) + v_i h_j w_{i,j}\rangle$ .

**end for**

$\sum_{v,h} \sqrt{Q(v,h)} |v\rangle |h\rangle |E(v,h)\rangle \rightarrow \sum_{v,h} \sqrt{Q(v,h)} |v\rangle |h\rangle |E(v,h)\rangle \left( \sqrt{\frac{e^{-E(v,h)}}{Z_{\text{MF}} \kappa}} |1\rangle + \sqrt{1 - \frac{e^{-E(v,h)}}{Z_{\text{MF}} \kappa}} |0\rangle \right)$ .

**end function**

---



---

**Algorithm 2** Quantum algorithm for generating states that can be measured to estimate the expectation value over the data.

---

**Input:** Model weights  $w$ , visible biases  $b$ , hidden biases  $d$ , edge set  $E$  and  $\kappa_x$ , training vector  $x$ .

**Output:** Quantum state that can be measured to obtain the correct Gibbs state for a (deep) Boltzmann machine with the visible units clamped to  $x$ .

---

**function** QGENDATASTATE( $w, b, d, E, \kappa_x, x$ )

  Compute vectors of mean-field parameters  $\nu$  from  $w, b$  and  $d$  with visible units clamped to  $x$ .

  Compute the mean-field partition function  $Z_{x,\text{MF}}$ .

**for**  $i = 1 : n_v$  **do**

$\sum_h \sqrt{Q(x,h)} |x\rangle |h\rangle |E(x,h)\rangle \rightarrow \sum_h \sqrt{Q(x,h)} |x\rangle |h\rangle |E(x,h) + x_i b_i\rangle$ .

**end for**

**for**  $j = 1 : n_h$  **do**

$\sum_h \sqrt{Q(x,h)} |x\rangle |h\rangle |E(x,h)\rangle \rightarrow \sum_h \sqrt{Q(x,h)} |x\rangle |h\rangle |E(x,h) + h_j d_j + \ln(\nu_j^{h_j} (1 - \nu_j)^{1-h_j})\rangle$ .

**end for**

**for**  $(i,j) \in E$  **do**

$\sum_h \sqrt{Q(x,h)} |x\rangle |h\rangle |E(x,h)\rangle \rightarrow \sum_h \sqrt{Q(x,h)} |x\rangle |h\rangle |E(x,h) + x_i h_j w_{i,j}\rangle$ .

**end for**

$\sum_h \sqrt{Q(x,h)} |x\rangle |h\rangle |E(x,h)\rangle \rightarrow \sum_h \sqrt{Q(x,h)} |x\rangle |h\rangle |E(x,h)\rangle \left( \sqrt{\frac{e^{-E(x,h)}}{Z_{x,\text{MF}} \kappa_x}} |1\rangle + \sqrt{1 - \frac{e^{-E(x,h)}}{Z_{x,\text{MF}} \kappa_x}} |0\rangle \right)$ .

**end function**

---

The approach to the state preparation problem used in [Lemma 2](#) is similar to that of [\[27\]](#), with the exception that we use a mean-field approximation rather than the infinite temperature Gibbs state as our initial state. This choice of initial state is important because the success probability of the state preparation process depends on the distance between the initial state and the target state. For machine learning applications, the inner product between the Gibbs state and the infinite temperature Gibbs state is often exponentially small; whereas we find in [Section VII C](#) that the mean-field and the Gibbs states typically have large overlaps.

The following lemma is a more general version of [Lemma 2](#) that shows that if a insufficiently large value of  $\kappa$  is used then the state preparation algorithm can still be employed, but at the price of reduced fidelity with the ideal coherent Gibbs state.

**Lemma 3.** *If we relax the assumptions of [Lemma 2](#) such that  $\kappa Q(v,h) \geq e^{-E(v,h)}/Z_{\text{MF}}$  for all  $(v,h) \in \text{good}$  and  $\kappa Q(v,h) < e^{-E(v,h)}/Z_{\text{MF}}$  for all  $j \in \text{bad}$  and  $\sum_{(v,h) \in \text{bad}} (e^{-E(v,h)} - Z_{\text{MF}} \kappa Q(v,h)) \leq \epsilon Z$ , then a state can be prepared*

that has fidelity at least  $1 - \epsilon$  with the target Gibbs state with probability at least  $Z(1 - \epsilon)/(\kappa Z_{\text{MF}})$ .

*Proof.* Let our protocol be that used in [Lemma 2](#) with the modification that the rotation is only applied if  $e^{-E(v,h)}/Z_{\text{MF}}\kappa \leq 1$ . This means that prior to the measurement of the register that projects the state onto the success or failure branch, the state is

$$\sum_{(v,h) \in \text{good}} \sqrt{Q(v,h)} |v\rangle |h\rangle \left( \sqrt{\frac{e^{-E(v,h)}}{Z_{\text{MF}}\kappa Q(v,h)}} |1\rangle + \sqrt{1 - \frac{e^{-E(v,h)}}{Z_{\text{MF}}\kappa Q(v,h)}} |0\rangle \right) + \sum_{(v,h) \in \text{bad}} \sqrt{Q(v,h)} |v\rangle |h\rangle |1\rangle \quad (21)$$

The probability of successfully preparing the approximation to the state is then

$$\sum_{(v,h) \in \text{good}} \frac{e^{-E(v,h)}}{\kappa Z_{\text{MF}}} + \sum_{(v,h) \in \text{bad}} Q(v,h) = \frac{Z - (\sum_{(v,h) \in \text{bad}} e^{-E(v,h)} - \sum_{(v,h) \in \text{bad}} \kappa Z_{\text{MF}} Q(v,h))}{Z_{\text{MF}}\kappa} \geq \frac{Z(1 - \epsilon)}{\kappa Z_{\text{MF}}}. \quad (22)$$

The fidelity of the resultant state with the ideal state  $\sum_{v,h} \sqrt{e^{-E(v,h)}/Z} |v\rangle |h\rangle$  is

$$\frac{\sum_{(v,h) \in \text{good}} e^{-E(v,h)} + \sum_{(v,h) \in \text{bad}} \sqrt{Q(v,h)Z_{\text{MF}}\kappa} e^{-E(v,h)}}{\sqrt{Z(\sum_{(v,h) \in \text{good}} e^{-E(v,h)} + \sum_{(v,h) \in \text{bad}} Q(v,h))}} \geq \frac{\sum_{(v,h) \in \text{good}} e^{-E(v,h)} + \sum_{(v,h) \in \text{bad}} Q(v,h)}{\sqrt{Z(\sum_{(v,h) \in \text{good}} e^{-E(v,h)} + \sum_{(v,h) \in \text{bad}} Q(v,h))}}, \quad (23)$$

since  $Q(v,h)Z_{\text{MF}}\kappa \leq e^{-E(v,h)}$  for all  $(v,h) \in \text{bad}$ . Now using the assumption that  $\sum_{(v,h) \in \text{bad}} (e^{-E(v,h)} - Z_{\text{MF}}\kappa Q(v,h)) \leq \epsilon Z$ , we have that the fidelity is bounded above by

$$\frac{\sqrt{\sum_{(v,h) \in \text{good}} e^{-E(v,h)} + \sum_{(v,h) \in \text{bad}} Q(v,h)}}{\sqrt{Z}} \geq \sqrt{1 - \epsilon} \geq 1 - \epsilon. \quad (24)$$

□

The corresponding algorithms are outlined in [Algorithm 1](#) and [Algorithm 2](#), for preparing the state required for the model expectation and the data expectation, respectively.

## V. GRADIENT CALCULATION BY SAMPLING

Our first algorithm for estimating the gradients of  $O_{\text{ML}}$  involves preparing the Gibbs state from the mean-field state and then drawing samples from the resultant distribution in order to estimate the expectation values required in [\(4\)](#). We also optimize this algorithm by utilizing a quantum algorithm known as amplitude amplification [\[28\]](#) (a generalization of Grover's search algorithm [\[29\]](#)) which quadratically reduces the mean number of repetitions needed to draw a sample from the Gibbs distribution using the approach in [Lemma 2](#) or [Lemma 3](#). We state the performance of this algorithm in the following theorem.

**Theorem 1.** *There exists a quantum algorithm that can estimate the gradient of  $O_{\text{ML}}$  using  $N_{\text{train}}$  samples for a Boltzmann machine on a connected graph with  $E$  edges. The mean number of quantum operations required by algorithm to compute the gradient is*

$$\tilde{O} \left( N_{\text{train}} E \sqrt{\kappa + \sum_{v \in \mathcal{X}_{\text{train}}} \kappa_v} \right),$$

where  $\kappa_v$  is the value of  $\kappa$  that corresponds to the Gibbs distribution when the visible units are clamped to  $v$  and  $f \in \tilde{O}(g)$  implies  $f \in O(g)$  up to polylogarithmic factors.

*Proof.* We use [Algorithm 3](#) to compute the required gradients. It is straightforward to see from [Lemma 2](#) that [Algorithm 3](#) draws  $N_{\text{train}}$  samples from the Boltzmann machine and then estimates the expectation values in [\(4\)](#) using the expectation values computed over these samples. The subroutines that generate these states, `qGenModelState` and `qGenDataState`, given in [Algorithm 1](#) and [Algorithm 2](#), represent the only quantum processing in this algorithm.

The number of times the subroutines must be called on average before a success is observed is given by the mean of a geometric distribution with success probability given by [Lemma 2](#) that is at least

$$\min \left\{ \frac{Z}{\kappa Z_{\text{MF}}}, \min_x \frac{Z_x}{\kappa_x Z_{x,\text{MF}}} \right\}. \quad (25)$$

[Lemma 1](#) gives us that  $Z > Z_{\text{MF}}$  and hence the probability of success satisfies

$$\min \left\{ \frac{Z}{\kappa Z_{\text{MF}}}, \min_v \frac{Z_x}{\kappa_x Z_{x,\text{MF}}} \right\} \geq \frac{1}{\kappa + \max_v \kappa_v}. \quad (26)$$

Normally, [\(26\)](#) implies that preparation of the Gibbs state would require  $O(\kappa + \max_v \kappa_v)$  calls to [Algorithm 1](#) and [Algorithm 2](#) on average, but the quantum amplitude amplification algorithm [\[28\]](#) reduces the average number of repetitions needed before a success is obtained to  $O(\sqrt{\kappa + \max_v \kappa_v})$ . [Algorithm 3](#) therefore requires an average number of calls to `qGenModelState` and `qGenDataState` that scale as  $O(N_{\text{train}} \sqrt{\kappa + \max_v \kappa_v})$ .

[Algorithm 1](#) and [Algorithm 2](#) require preparing the mean-field state, computing the energy of a configuration  $(v, h)$ , and performing a controlled rotation. Assuming that the graph is connected, the number of hidden and visible units are  $O(E)$ . Since the cost of synthesizing single qubit rotations to within error  $\epsilon$  is  $O(\log(E/\epsilon))$  [\[23–25\]](#) and the cost of computing the energy is  $O(E \text{ polylog}(E/\epsilon))$  it follows that the cost of these algorithms is  $\tilde{O}(E)$ . Thus the expected cost of [Algorithm 3](#) is  $\tilde{O}(N_{\text{train}} E \sqrt{\kappa + \max_v \kappa_v})$  as claimed.  $\square$

In contrast, the number of operations and queries to  $U_O$  required to estimate the gradients using greedy layer-by-layer optimization scales as [\[3\]](#)

$$\tilde{O}(N_{\text{train}} \ell E), \quad (27)$$

where  $\ell$  is the number of layers in the deep Boltzmann machine. Assuming that  $\kappa$  is a constant, it follows that the quantum sampling approach provides an asymptotic advantage for training deep networks. In practice, the two approaches are difficult to directly compare because they both optimize different objective functions and thus the qualities of the resultant trained models will differ. It is reasonable to expect, however, that the quantum approach will tend to find superior models because it optimizes the maximum-likelihood objective function up to sampling error due to taking finite  $N_{\text{train}}$ .

Note that [Algorithm 3](#) has an important advantage over many existing quantum machine learning algorithms [\[15, 17–19\]](#): *it does not require that the training vectors are stored in quantum memory*. It requires only  $n_h + n_v + 1 + \lceil \log_2(1/\mathcal{E}) \rceil$  qubits if a numerical precision of  $\mathcal{E}$  is needed in the evaluation of the  $E(v, h) - \log(Q(v, h))$ . This means that a demonstration of this algorithm that would not be classically simulatable could be performed with fewer than 100 qubits, assuming that 32 bits of precision suffices for the energy. In practice though, additional qubits will likely be required to implement the required arithmetic on a quantum computer. Recent developments in quantum rotation synthesis could, however, be used to remove the requirement that the energy is explicitly stored as a qubit string [\[30\]](#), which may substantially reduce the space requirements of this algorithm. Below we consider the opposite case: the quantum computer can coherently access the database of training data via an oracle. The algorithm requires more qubits (space), however it in turn quadratically reduces the number of samples required for learning.

## VI. TRAINING VIA QUANTUM AMPLITUDE ESTIMATION

We now consider a different learning environment, one in which the user has access to the training data via a quantum oracle which could represent either an efficient quantum algorithm that provides the training data (such as another Boltzmann machine used as a generative model) or a quantum database that stores the memory via a binary access tree [\[22, 31\]](#), such as a quantum Random Access Memory (qRAM) [\[31\]](#).

If we denote the training set as  $\{x_i | i = 1, \dots, N_{\text{train}}\}$ , then the oracle is defined as a unitary operation as follows:

**Definition 3.**  $U_O$  is a unitary operation that performs for any computational basis state  $|i\rangle$  and any  $y \in \mathbb{Z}_2^{n_v}$

$$U_O |i\rangle |y\rangle := |i\rangle |y \oplus x_i\rangle,$$

where  $\{x_i | i = 1, \dots, N_{\text{train}}\}$  is the training set and  $x_i \in \mathbb{Z}_2^{n_v}$ .

---

**Algorithm 3** Quantum algorithm for estimating the gradient of  $O_{\text{ML}}$ .

---

**Input:** Initial model weights  $w$ , visible biases  $b$ , hidden biases  $d$ , edge set  $E$  and  $\kappa$ , a set of training vectors  $x_{\text{train}}$ , a regularization term  $\lambda$ , and a learning rate  $r$ .

**Output:** Three arrays containing gradients of weights, hidden biases and visible biases: `gradMLw`, `gradMLb`, `gradMLd`.

---

```

for  $i = 1 : N_{\text{train}}$  do
  success  $\leftarrow 0$ 
  while success = 0 do
     $|\psi\rangle \leftarrow \text{qGenModelState}(w, b, d, E, \kappa)$ 
    success  $\leftarrow$  result of measuring last qubit in  $|\psi\rangle$ 
  end while
   $\text{modelVUnits}[i] \leftarrow$  result of measuring visible qubit register in  $|\psi\rangle$ .
   $\text{modelHUnits}[i] \leftarrow$  result of measuring hidden unit register in  $|\psi\rangle$  using amplitude amplification.
  success  $\leftarrow 0$ 
  while success = 0 do
     $|\psi\rangle \leftarrow \text{qGenDataState}(w, b, d, E, \kappa, x_{\text{train}}[i])$ .
    success  $\leftarrow$  result of measuring last qubit in  $|\psi\rangle$  using amplitude amplification.
  end while
   $\text{dataVUnits}[i] \leftarrow$  result of measuring visible qubit register in  $|\psi\rangle$ .
   $\text{dataHUnits}[i] \leftarrow$  result of measuring hidden unit register in  $|\psi\rangle$ .
end for
for each visible unit  $i$  and hidden unit  $j$  do
   $\text{gradMLw}[i, j] \leftarrow r \left( \frac{1}{N_{\text{train}}} \sum_{k=1}^{N_{\text{train}}} (\text{dataVUnits}[k, i] \text{dataHUnits}[k, j] - \text{modelVUnits}[k, i] \text{modelHUnits}[k, j]) - \lambda w_{i, j} \right)$ .
   $\text{gradMLb}[i] \leftarrow r \left( \frac{1}{N_{\text{train}}} \sum_{k=1}^{N_{\text{train}}} (\text{dataVUnits}[k, i] - \text{modelVUnits}[k, i]) \right)$ .
   $\text{gradMLd}[j] \leftarrow r \left( \frac{1}{N_{\text{train}}} \sum_{k=1}^{N_{\text{train}}} (\text{dataHUnits}[k, j] - \text{modelHUnits}[k, j]) \right)$ .
end for

```

---

A single quantum access to  $U_O$  is sufficient to prepare a uniform distribution over all the training data

$$U_O \left( \frac{1}{N_{\text{train}}} \sum_{i=1}^{N_{\text{train}}} |i\rangle |0\rangle \right) = \frac{1}{N_{\text{train}}} \sum_{i=1}^{N_{\text{train}}} |i\rangle |x_i\rangle. \quad (28)$$

The state  $\frac{1}{N_{\text{train}}} \sum_{i=1}^{N_{\text{train}}} |i\rangle |0\rangle$  can be efficiently prepared using quantum techniques [19] and so the entire procedure is efficient.

At first glance, the ability to prepare a superposition over all data from the training set seems to be a powerful resource. However, a similar probability distribution can also be generated classically using one query by picking a random training vector. More sophisticated approaches are needed if we wish to leverage such quantum superpositions of the training data. [Algorithm 4](#) utilizes such superpositions to provide advantages, under certain circumstances, for computing the gradient. The performance of this algorithm is given in the following theorem.

**Theorem 2.** *There exists a quantum algorithm that can compute  $r \frac{\partial O_{\text{ML}}}{\partial w_{ij}}$ ,  $r \frac{\partial O_{\text{ML}}}{\partial b_i}$  or  $r \frac{\partial O_{\text{ML}}}{\partial d_j}$  for a Boltzmann machine on a connected graph with  $E$  edges to within error  $\delta$  using an expected number of queries to  $U_O$  that scales as*

$$\tilde{O} \left( \frac{\kappa + \max_v \kappa_v}{\delta} \right),$$

and a number of quantum operations that scales as

$$\tilde{O} \left( \frac{E(\kappa + \max_v \kappa_v)}{\delta} \right),$$

for constant learning rate  $r$ .

[Algorithm 4](#) requires the use of the amplitude estimation [28] algorithm, which provides a quadratic reduction in the number of samples needed to learn the probability of an event occurring, as stated in the following theorem.

**Theorem 3** (Brassard, Høyer, Mosca and Tapp). *For any positive integer  $L$ , the amplitude estimation algorithm of takes as input a quantum algorithm that does not use measurement and with success probability  $a$  and outputs  $\tilde{a}$*

( $0 \leq \tilde{a} \leq 1$ ) such that

$$|\tilde{a} - a| \leq \frac{\pi(\pi + 1)}{L}$$

with probability at least  $8/\pi^2$ . It uses exactly  $L$  iterations of Grover's algorithm. If  $a = 0$  then  $\tilde{a} = 0$  with certainty, and if  $a = 1$  and  $L$  is even, then  $\tilde{a} = 1$  with certainty.

This result is central to the proof of [Theorem 2](#) which we give below.

*Proof of [Theorem 2](#).* [Algorithm 4](#) computes the derivative of  $O_{\text{ML}}$  with respect to the weights. The algorithm can be trivially adapted to compute the derivatives with respect to the biases. The first step in the algorithm prepares a uniform superposition of all training data and then applies  $U_O$  to it. The result of this is

$$\frac{1}{\sqrt{N_{\text{train}}}} \sum_{p=1}^{N_{\text{train}}} |p\rangle |x_p\rangle, \quad (29)$$

as claimed.

Any quantum algorithm that does not use measurement is linear and hence applying `qGenDataState` ([Algorithm 2](#)) to (29) yields

$$\begin{aligned} & \frac{1}{\sqrt{N_{\text{train}}}} \sum_{p=1}^{N_{\text{train}}} |p\rangle |x_p\rangle \sum_h \sqrt{Q(x_p, h)} |h\rangle |\mathcal{P}(x_p, h)\rangle \left( \sqrt{1 - \mathcal{P}(x_p, h)} |0\rangle + \sqrt{\mathcal{P}(x_p, h)} |1\rangle \right) \\ & := \frac{1}{\sqrt{N_{\text{train}}}} \sum_{p=1}^{N_{\text{train}}} |p\rangle |x_p\rangle \sum_h \sqrt{Q(x_p, h)} |h\rangle |\mathcal{P}(x_p, h)\rangle |\chi(x_p, h)\rangle. \end{aligned} \quad (30)$$

If we consider measuring  $\chi = 1$  to be success then [Theorem 3](#) gives us that  $\tilde{O}((\kappa + \max_v \kappa_v)/\Delta)$  preparations of (30) are needed to learn  $P(\text{success}) = P(\chi = 1)$  to within relative error  $\Delta/8$  with high probability. This is because  $P(\text{success}) \geq 1/(\kappa + \max_v \kappa_v)$ . Similarly, we can also consider success to be the event where the  $i^{\text{th}}$  visible unit is 1 and the  $j^{\text{th}}$  hidden unit is one and a successful state preparation is measured. This marking process is exactly the same as the previous case, but requires a Toffoli gate. Thus  $P(v_i = h_j = \chi = 1)$  can be learned within relative error  $\Delta/8$  using  $\tilde{O}((\kappa + \max_v \kappa_v)/\Delta)$  preparations. It then follows from the laws of conditional probability that

$$\langle v_i h_j \rangle_{\text{data}} = P([x_p]_i = h_j = 1 | \chi = 1) = \frac{P([x_p]_i = h_j = \chi = 1)}{P(\chi = 1)}, \quad (31)$$

can be calculated from these values as claimed.

In order to ensure that the total error in  $\langle v_i h_j \rangle_{\text{data}}$  is at most  $\Delta$ , we need to bound the error in the quotient in (31). It can be seen that for  $\Delta < 1/2$ ,

$$\left| \frac{P([x_i]_j = h_k = \chi = 1)(1 \pm \Delta/8)}{P(\chi = 1)(1 \pm \Delta/8)} - \frac{P([x_i]_j = h_k = \chi = 1)}{P(\chi = 1)} \right| \leq \frac{\Delta P([x_i]_j = h_k = \chi = 1)}{P(\chi = 1)} \leq \Delta. \quad (32)$$

Therefore the algorithm gives  $\langle v_i h_j \rangle_{\text{data}}$  within error  $\Delta$ .

The exact same steps can be repeated using [Algorithm 1](#) instead of [Algorithm 2](#) as the state preparation subroutine used in amplitude estimation. This allows us to compute  $\langle v_i h_j \rangle_{\text{data}}$  within error  $\Delta$  using  $\tilde{O}(1/\Delta)$  state preparations. The triangle inequality shows that the maximum error incurred from approximating  $\langle v_i h_j \rangle_{\text{data}} - \langle v_i h_j \rangle_{\text{model}}$  is at most  $2\Delta$ . Therefore, since a learning rate of  $r$  is used in [Algorithm 4](#), the overall error in the derivative is at most  $2\Delta r$ . If we pick  $\Delta = \delta/(2r)$  then we see that the overall algorithm requires  $\tilde{O}(1/\delta)$  state preparations for constant  $r$ .

Each state preparation requires one query to  $U_O$  and  $\tilde{O}(E)$  operations assuming that the graph that underlies the Boltzmann machine is connected. This means that the expected query complexity of the algorithm is  $\tilde{O}((\kappa + \max_v \kappa_v)/\delta)$  and the number of circuit elements required is  $\tilde{O}((\kappa + \max_v \kappa_v)E/\delta)$  as claimed.  $\square$

There are two qualitative differences between this approach and that of [Algorithm 3](#). The first is that the algorithm provides detailed information about one direction of the gradient, whereas the samples from [Algorithm 3](#) provide limited information about every direction. It may seem reasonable that if amplitude estimation is used to learn  $\langle v_i h_j \rangle$  then  $\langle v_k h_\ell \rangle$  could be estimated by sampling from the remaining qubits. The problem is that amplitude estimation

---

**Algorithm 4** Quantum algorithm for computing gradient of weights using amplitude estimation for use in training a deep Boltzmann machine.

---

**Input:** Initial model weights  $w$ , visible biases  $b$ , hidden biases  $d$ , edge set  $E$  and  $\kappa$ , a set of training vectors  $x_{\text{train}}$ , a regularization term  $\lambda$ ,  $1/2 \geq \Delta > 0$ , a learning rate  $r$ , and a specification of edge  $(i, j)$ .

**Output:**  $r \frac{\partial \mathcal{O}_{\text{ML}}}{\partial w_{ij}}$  calculated to within error  $2r\Delta$ .

---

Call  $U_O$  once to prepare state  $|\psi\rangle \leftarrow \frac{1}{\sqrt{N_{\text{train}}}} \sum_{p \in x_{\text{train}}} |p\rangle |x_p\rangle$ .

$|\psi\rangle \leftarrow \text{qGenDataState}(w, b, d, E, \kappa, |\psi\rangle)$ .  $\triangleright$  Apply [Algorithm 2](#) using a superposition over  $x_p$  rather than a single value.

Use amplitude estimation on state preparation process for  $|\psi\rangle$  to learn  $P([x_p]_i = h_j = \text{success} = 1)$  within error  $\Delta/8$ .

Use amplitude estimation on state preparation process for  $|\psi\rangle$  to learn  $P(\text{success} = 1)$  within error  $\Delta/8$ .

$\langle v_i h_j \rangle_{\text{data}} \leftarrow \frac{P([x_p]_i = h_j = \text{success} = 1)}{P(\text{success} = 1)}$ .

Use amplitude estimation in exact same fashion on  $\text{qGenModelState}(w, b, d, E, \kappa)$  to learn  $\langle v_i h_j \rangle_{\text{model}}$ .

$\frac{\partial \mathcal{O}_{\text{ML}}}{\partial w_{ij}} \leftarrow r (\langle v_i h_j \rangle_{\text{data}} - \langle v_i h_j \rangle_{\text{model}})$

---

creates biases in these measurements and so the correct way to use this evidence to update the user’s confidence about the remaining components of the gradient is unclear. The second difference is that the algorithm does not use amplitude amplification to reduce the effective value of  $\kappa$ . This is because amplitude amplification is only known to give a quadratic advantage if used in an algorithm that utilizes measurement and feedback unless the probability of success is known. Since amplitude estimation cannot be used on subroutines that utilize measurement in a non-trivial fashion, the two methods cannot be used simultaneously. It is not obvious how to optimize [Algorithm 4](#) to have the same scaling with  $\kappa$  and  $E$  as [Algorithm 3](#).

This process can be repeated for each of the components of the gradient vector in order to perform an update of the weights and biases of the Boltzmann machine.

**Corollary 1.** *The number of quantum operations needed to compute the gradient of  $\mathcal{O}_{\text{ML}}$  using [Algorithm 4](#) for a Boltzmann machine on a connected graph scales as*

$$\tilde{O} \left( \frac{E^2 (\kappa + \max_v \kappa_v)}{\delta} \right),$$

if the learning rate  $r$  is a constant.

*Proof.* The proof is a trivial consequence of using the result of [Theorem 2](#)  $O(E)$  times to compute each of the components of the gradient vector.  $\square$

Unlike the prior algorithm, it is very difficult to meaningfully compare the costs in [Corollary 1](#) to those incurred with training under contrastive divergence. This is because [Algorithm 4](#) uses quantum superposition to compute the relevant expectation values using all the training data simultaneously. Thus each component of the derivative operator is computed using the entire set of data, and it is better to instead consider the run time as a function of the estimation error rather than the number of training vectors. Thus the query complexity of does not depend in a clear way on  $N_{\text{train}}$ .

Although the query complexity is independent of the number of training vectors, in order to assess the cost of this algorithm in practical examples we also need to include the costs of instantiating the oracle. We consider three cases. If each oracle implements an efficiently computable function then the space- and time-complexities of implementing the oracle is polylogarithmic in  $N_{\text{train}}$ . On the other hand, if the data can only be accessed via a lookup table (as is true in most machine learning problems) then a quantum computer that allows parallel execution can implement the oracle in time  $O(\text{polylog}(N_{\text{train}}))$  using memory  $O(N_{\text{train}})$ . If on the other hand the quantum computer only can process information serially then  $\Theta(N_{\text{train}})$  space and time are required to implement an oracle query using a database of training vectors stored as a qubit string in the quantum computer. The lower bound follows from lower bounds on the parity function that show  $\Theta(N)$  queries to the bits in this database are required to determine the parity of a  $N$  qubit string. This shows that the dependence on the number of training vectors re-emerges depending on problem- and architecture-specific issues.

The quadratic scaling with  $E$  means that [Algorithm 4](#) may not be preferable to [Algorithm 3](#) for learning all of the weights. On the other hand, [Algorithm 4](#) can be used to improve gradients estimated using the prior method. The idea is to begin with a preliminary gradient estimation step using the direct gradient estimation method while using  $O(\sqrt{N_{\text{train}}})$  randomly selected training vectors. Then the gradient is estimated by breaking the results into smaller

groups and computing the mean and the variance of each component of the gradient vector over each of the subgroups. The components of the gradients with the largest uncertainty can then be learned with error that is comparable to the sampling error incurred by only using  $N_{\text{train}}$  training examples in contrastive divergence training by using [Algorithm 4](#) with  $\delta \sim 1/\sqrt{N_{\text{train}}}$  to estimate them. Since the two costs are asymptotically comparable, this approach allows the benefits of both approaches to be used in cases where the majority of the uncertainty in the gradient comes from a small number of components.

## VII. NUMERICAL EXPERIMENTS

In this section we quantify the differences between training Boltzmann machines using contrastive divergence (see [Appendix B](#) for a brief review of contrastive divergence) and training them by optimizing  $O_{\text{ML}}$  using [Algorithm 3](#) or [Algorithm 4](#). Specifically, we address the following questions:

1. Does noise in the gradients affect the quality of optima found by training using [Algorithm 3](#) or [Algorithm 4](#)? If so, by how much?
2. What are typical values of  $\kappa$  for real-world learning problems when using these algorithms?
3. How do the models learned using one step CD (CD-1) training differ from those learned using quantum  $O_{\text{ML}}$  optimization?

The first two questions examine the performance of our quantum algorithms in the presence of errors in the gradient and errors in the mean-field approximation. The last question quantifies how models learned using contrastive divergence differ from those learned using  $O_{\text{ML}}$  optimization. Finally, we also study the performance of full Boltzmann machines when trained under  $O_{\text{ML}}$ .

### A. Data and Methodology

The cost of exactly computing the ML objective function grows exponentially with the number of units in the Boltzmann machine. Computational restrictions therefore place severe limitations on the size of training sets and models that we can study in numerical experiments. In practice, we are computationally limited to models with at most 20 visible and hidden units. We train the following experiments on dRBMs with  $\ell$  layers,  $\ell \in \{2, 3\}$ ,  $n_h$  hidden units,  $n_h \in \{2, \dots, 8\}$ , and  $n_v$  visible units,  $n_v \in \{4, \dots, 12\}$ .

Our training data is generated synthetically and consists of bit strings based on four distinct functions:

$$\begin{aligned}
 [x_1]_j &= \begin{cases} 1 & j = 1, \dots, \lfloor n_v/2 \rfloor \\ 0 & \text{otherwise} \end{cases} \\
 [x_2]_j &= \begin{cases} 0 & j = 1, \dots, \lfloor n_v/2 \rfloor \\ 1 & \text{otherwise} \end{cases} \\
 [x_3]_j &= j \pmod 2 \\
 [x_4]_j &= j + 1 \pmod 2.
 \end{aligned} \tag{33}$$

We add Bernoulli noise  $\mathcal{N}$  to each of the bits in the bit string to increase the size of the training sets. In particular, we take each of the four patterns in [\(33\)](#) and flip each bit with probability  $\mathcal{N}$ . We use 10,000 training examples in each of our numerical experiments and these vectors contain 4,  $\dots$ , 12 binary features. Our task is to infer a generative model for these four vectors. A simple generalization of this approach would allow the dRBM to learn a decoder for these four codewords being sent over a noisy channel.

We train the dRBM model using gradient ascent with (1) contrastive divergence to approximate the gradients and (2) ML-objective optimization (ML) using techniques of [Algorithm 3](#) or [Algorithm 4](#). The desired objective function in both cases is  $O_{\text{ML}}$ . Since different approximations to the gradient result in learning different local optima, even if the same initial conditions are used in both instances, it is potentially unfair to directly compare the optima vectors found using the two training techniques. We consider two methods of comparison. First, we verify that our results lie approximately in an optima of  $O_{\text{ML}}$  with high probability by using the approach of Donmez, Svore and Burges [\[32\]](#). For each proposed optima, we perform many perturbations about the point, fixing all parameters while perturbing one, and repeating many times for each parameter, and then compare the difference in the value of the objective functions at the original and perturbed points. This allows us to say, with fixed confidence, that the probability of

	First Optimizer	Second Optimizer
CD–ML	CD–1	Gradient ascent on ML objective
ML–CD	BFGS on ML objective	CD–1
ML–ML	BFGS on ML objective	Noisy gradient ascent on ML objective.

TABLE I: Numerical experiments considered.

the objective function decreasing in a randomly chosen direction is less than a cited value. We repeat this process 459 times with perturbations of size  $10^{-3}$ , which is sufficient to guarantee that the objective function will not increase in 99% of all randomly chosen directions for steps of size  $10^{-3}$ .

Second, we use a methodology similar to that used in [33]. We perform our experiments by running one algorithm until a local optima is found and then using this local optima as the initial configuration for the second algorithm. In this way we can compare the locations and quality of analogous local optima. We list the training combinations in Table I, which we denote CD–ML, ML–CD, and ML–ML corresponding to the optimizers used in the first and second steps of the comparison. A subtle point in considering such comparisons is determination of convergence. Contrastive divergence and other noisy gradient ascent algorithms (meaning gradient ascent where noise is added to the gradient calculation) do not converge to a single optima, but instead fluctuate about an approximate fixed point. For this reason we consider an algorithm to have converged when the running average of the value of  $O_{\text{ML}}$  varies by less than 0.001% after at least 10,000 training epochs with a learning rate of  $r = 0.01$ . We apply this stopping condition not only in our contrastive divergence calculations, but also when we determine the effect of introducing sampling noise into the gradient of the ML objective function. We typically optimize the ML objective function in the absence of noise using the Broyden–Fletcher–Goldfarb–Shanno algorithm (BFGS), but also use gradient ascent using discretized derivatives. In both cases, we choose our stopping condition to occur when an absolute error of  $10^{-7}$  in the ML objective function is obtained.

### B. Effect of noise in the gradient

We first determine whether a sufficiently accurate estimate of the gradient can be obtained from a small number of samples from a quantum device, for example when training using Algorithm 3 or Algorithm 4. Here, we train a single-layer RBM using ML–ML, with 6 visible units and 4 hidden units. We then proceed by computing the gradient of the ML objective function and add zero-mean Gaussian noise to the gradient vector. The training data, consisting of 10,000 training examples. A minimum of 10,000 training epochs were used for each data point and typically fewer than 20,000 epochs were required before the stopping condition (given in Section VII A) was met.

Figure 2 shows that the mean error in the values of the objective function scales quadratically with the noise in the gradient. This means that the gradient ascent algorithm is highly resilient to sampling noise in the components in the gradient and a relatively small value of  $\delta$ , such as  $\delta = 0.01$ , will suffice to yield local optima that are close to those found when  $\delta = 0$ . Therefore, small sampling errors will not be catastrophic for Algorithm 4.

### C. Errors due to mean-field approximation and the scaling of $\kappa$

Our quantum algorithm hinges upon the ability to prepare an approximation to the Gibbs state from a mean-field, or related, approximation. Lemma 2 and Lemma 3 shows that the success probability of the algorithm strongly depends on the value of  $\kappa$  chosen and that the accuracy of the derivatives will suffer if a value of  $\kappa$  is used that is too small or  $Z_{\text{MF}}$  differs substantially from  $Z$ . We analyze the results for random single-layer RBMs with 4, 6, 8 visible units and four hidden units. The value of the standard deviation is an important issue because the quality of the mean-field approximation is known to degrade if stronger weights (i.e., stronger correlations) are introduced to the model [34]. We take the weights to be normally distributed in the Boltzmann machine with zero mean and standard deviation a multiple of 0.1325, which we chose to match the standard deviation of the weight distribution empirically found for a 884 unit RBM that was trained to perform facial recognition tasks using contrastive divergence. The biases are randomly set according to a Gaussian distribution with zero mean and unit variance for all numerical experiments in this section.

Figure 3 shows that the value of  $\kappa$  needed to ensure that the distribution that results from applying Lemma 3 is close to the ideal distribution is not prohibitively large. In fact,  $\kappa < 10$  suffices to produce the state with zero error for all of the cases considered. Furthermore, we see that the value of  $\kappa$  is a slowly increasing function of the number of visible units in the RBM and the standard deviation of the weights used in the synthetic models. The fact that  $\kappa$  is an increasing function of the standard deviation is not necessarily problematic, however, as regularization often

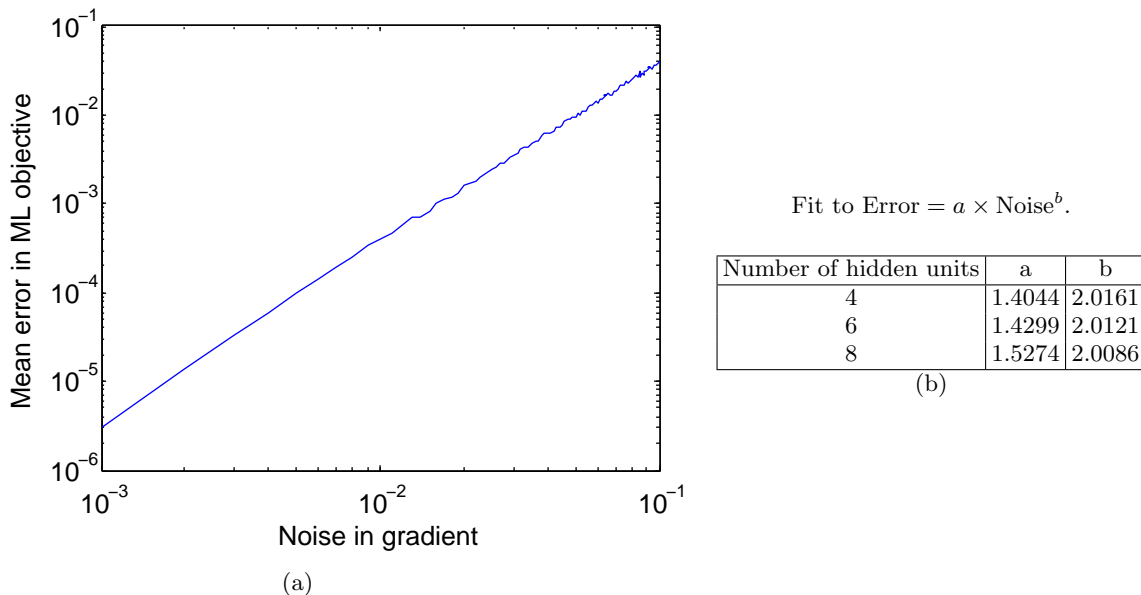


FIG. 2: (a) Mean discrepancy between ML-objective and ML found by initializing at ML-objective and introducing Gaussian noise to each component of the gradient computed. Data taken for  $6 \times 4$  unit RBM with  $\mathcal{N} = 0$  and 100 samples used in the average for each data point. (b) Results for  $6 \times n_h$  unit RBMs for  $n_h = 6, 8$  are qualitatively identical and strongly support a quadratic relationship between error and the noise in the gradient evaluation.

causes the standard deviation of the weights to be less than 1 in practical machine learning tasks. It is difficult though to extract the scaling of  $\kappa$  from this data as the value chosen depends sensitively on the cutoff point chosen for the residual probability.

We gain further intuition about the scaling of  $\kappa$  from the data in Figure 4, wherein we estimate an appropriate value of  $\kappa$  by taking  $\kappa_{\text{est}} = \sum_{v,h} P^2(v,h)/Q(v,h)$ . This estimate is clearly a lower bound on  $\max_{v,h} P(v,h)/Q(v,h)$ . Figure 4 reveals that  $\kappa_{\text{est}}$  scales roughly quadratically with the standard deviation of the edge weights and linearly with  $n_h$ . For cases where the standard deviation is large, deviations from this scaling appear. These deviations signal the breakdown of the mean-field approximation and may ultimately prevent efficient learning. However, in cases where the edge weights are modestly small we expect from this data and that in Figure 3 that our algorithms will remain tractable.

The quantity  $\kappa$  is small because the mean-field approximation is very close to the true Gibbs state for cases where the edge weights are small. This can be seen from the Table in Figure 3(d) and Figure 5, which give the mean values of the KL-divergence between the mean-field approximation and the true Gibbs state for the random RBMs.  $\text{KL}(Q||P)$  tends to be less than 0.1 for realistic weight distributions, implying that the mean-field approximation will often be very close to the actual distribution. The KL-divergence is also the slack in the variational approximation to the log-partition function (see Appendix A). This means that the data in Figure 3 also shows that  $Z_{\text{MF}}$  will closely approximate  $Z$  for these small synthetic models.

There are two competing trends in the success probability. As the mean-field approximation begins to fail, we expect that  $\kappa$  will diverge. On the other hand, we also expect  $Z/Z_{\text{MF}}$  to increase as the KL-divergence between  $Q$  and  $P$  increase. We can better understand the scaling of the error by taking the scaling of  $Z/Z_{\text{MF}}$  into consideration.  $Z_{\text{MF}}$  is a variational approximation to the partition function that obeys  $\log(Z_{\text{MF}}) = \log(Z) - \text{KL}(Q||P)$ , which implies

$$P_{\text{success}} \geq \frac{Z}{Z_{\text{MF}}\kappa} = \frac{e^{\text{KL}(Q||P)}}{\kappa} \geq \frac{1}{\kappa}. \quad (34)$$

The data in Figure 3 and Figure 5 shows that  $\text{KL}(Q||P)$  empirically scales as  $O(\sigma^2(w_{i,j})E)$ , where  $E$  is the number of edges in the graph and  $\sigma(w_{i,j})$  is the standard deviation in the weights of the synthetic models. Thus we expect that (a)  $P_{\text{success}} \approx 1/\kappa$  if  $\sigma^2(w_{i,j}) \in O(1/E)$  and (b)  $\kappa - 1 \in O(\sigma^2(w_{i,j})E)$  for  $\sigma^2(w_{i,j})E \ll 1$ . Thus our algorithms should be efficient if  $\sigma^2(w_{i,j})E$  is small for models that typically emerge in the training process.

We investigate this issue in Figure 6 where we compute the typical distribution of weights for a RBM with 12 visible units and a variable number of hidden units. This allows us to examine the scaling with the number of edges for a relatively large RBM trained using contrastive divergence. Although the weights learned via contrastive divergence differ from those learned using our quantum algorithm, we will see in Section VIID that these differences are often

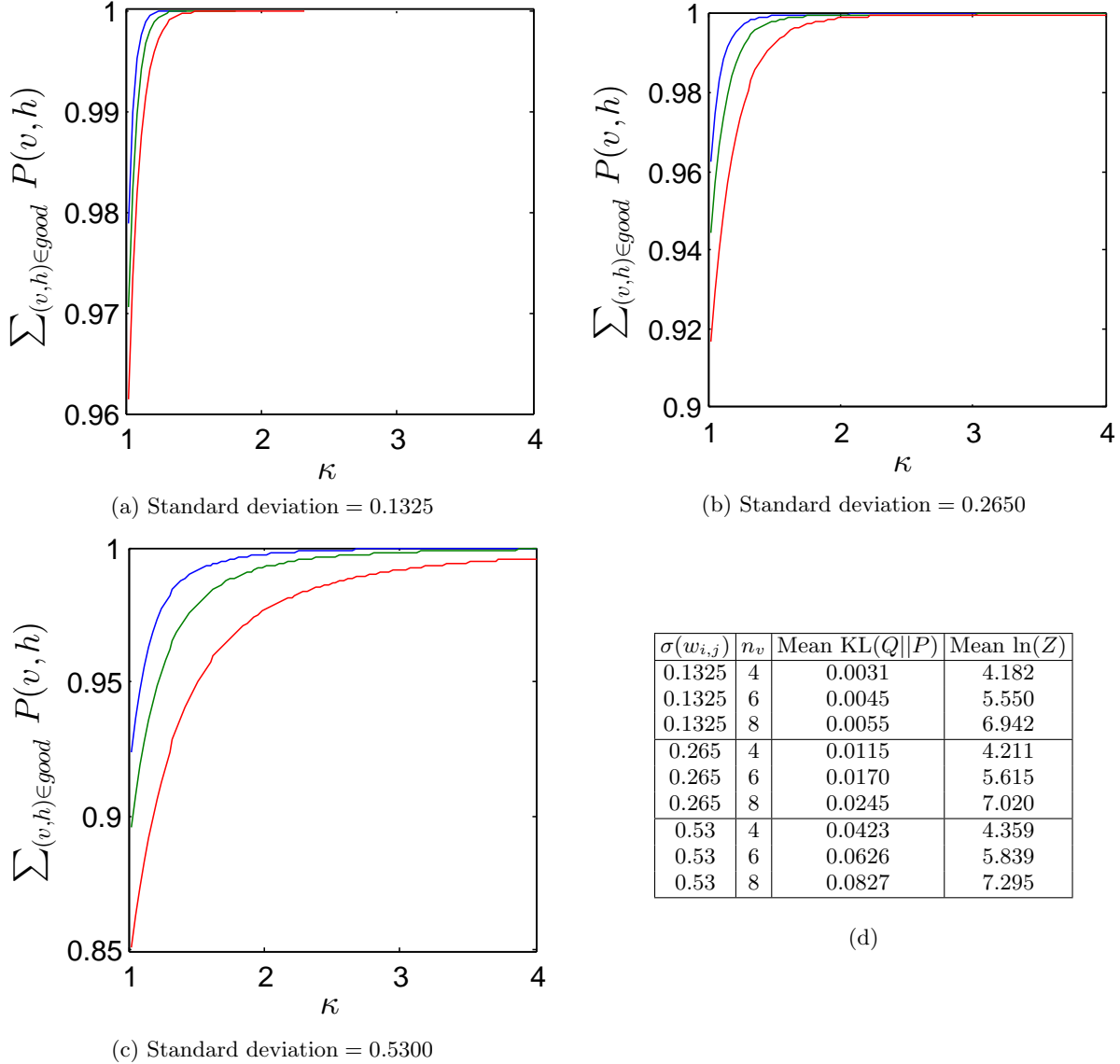


FIG. 3: Mean values of  $\kappa$  for synthetic  $n_v \times 4$  RBMs with weights chosen with weights chosen randomly according to a normal distribution with varying standard deviation for the weights and  $n = 4, 6, 8$  from top to bottom in each graph. Table (d) shows the values of the KL-divergence between the mean-field distribution and the Gibbs distribution for the data shown in (a), (b) and (c). Expectation values were found over 100 random instances.

small for RBMs and so contrastive divergence gives us a good estimate of how  $\sigma(w_{i,j})$  scales for large models that naturally arise through the training process. We note from Figure 6 that the standard deviation of the weights drops rapidly as more hidden units are added to the model. This is because regularization (i.e.,  $\lambda > 0$ ) provides a penalty for adding edges to the model. The variance in the weights decays faster than the  $\Theta(1/E)$  scaling that is expected to result in both high success probability and  $Z_{\text{MF}} \approx Z$ . Thus neither the scaling of  $\kappa$  nor the errors that arise from taking  $Z \approx Z_{\text{MF}}$  seem to be an obstacle for applying our methods (or natural generalizations thereof) to practical machine learning problems.

There is good reason to suspect that our algorithms cannot efficiently train all BMs. This is because the algorithms reduce the problem of training the system to the problem of preparing a Gibbs state. If we multiply the values of each weight and bias by a sufficiently large constant then we can cause the Gibbs state to closely approximate the ground state. The ground state energy could therefore be learned, with high probability, by measuring the resultant Gibbs state and computing the energy of the observed configuration using (2). Ground-state computation for non-planar Ising models is NP-complete, which means that our algorithm cannot be efficient in general unless  $\text{NP} \subseteq \text{BQP}$ , where BQP is the class of all decision problems that can be solved with high probability using a polynomial time calculation

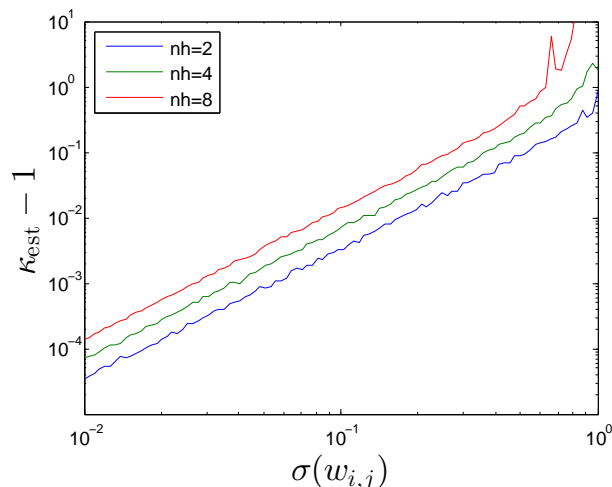


FIG. 4: Scaling of estimated  $\kappa$  as a function of the standard deviation of weights in synthetic RBMs with  $n_v = 4$  and Gaussian weights with zero mean and variance  $\sigma^2(w_{i,j})$ . The biases were set to be drawn from a Gaussian with zero mean and unit variance. Each data point is the average of 100 random RBMs and the data is consistent with an  $O(\sigma^2(w_{i,j})E)$  scaling for  $\sigma^2(w_{i,j})E \ll 1$ .

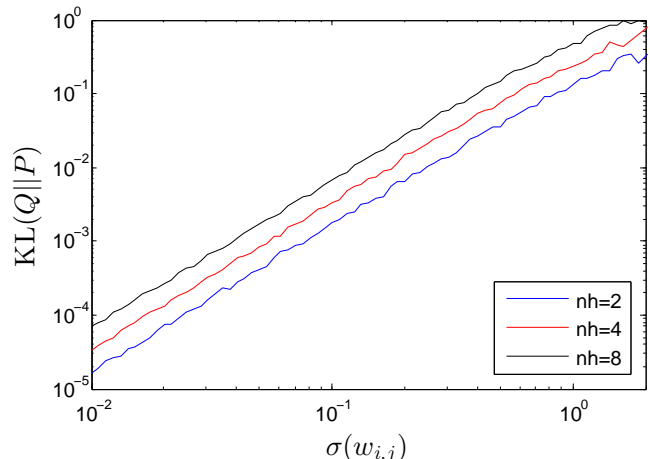


FIG. 5: Average KL-divergence as a function of the standard deviation of weights in synthetic RBMs with  $n_v = 4$  and Gaussian weights with zero mean and variance  $\sigma^2(w_{i,j})$ . The biases were set to be drawn from a Gaussian with zero mean and unit variance. Each data point is the average of 100 random RBMs and the data is consistent with an  $O(\sigma^2(w_{i,j})E)$  scaling.

on a quantum computer. It is widely conjectured that  $\text{NP} \not\subseteq \text{BQP}$  and as a result there are likely to be examples where our algorithms fail to be efficient. However, owing to the above experiments and the long history of using mean-field approximations in machine learning [7, 35, 38–40], such cases are likely to be atypical.

Several strategies can be used to combat low success probability for the preparation of the Gibbs state. In the event that the success probability is unacceptably low a more accurate estimate of the partition function than  $Z_{\text{MF}}$  can be used in the algorithm [8, 35–37]. Algorithm 3 can be used instead of Algorithm 4 to provide a quadratic advantage in the success probability. The value of  $\kappa$  chosen can also be decreased, as per Lemma 3. In extreme cases, the regularization constant can also be adjusted to combat the emergence of large weights in the training process; however, this runs the risk of producing a model that substantially underfits the data.

#### D. Comparison of CD-1 to ML learning

An important advantage of our quantum algorithms is that they provide an alternative to contrastive divergence for training deep restricted Boltzmann machines. We now investigate the question of whether substantial differences exist between the optima found by contrastive divergence and those found by optimization of the ML objective. We train using CD-ML on single-layer RBMs with up to 12 visible units and up to 6 hidden units and compute the distance between the optima found after first training with CD-1 and then training with ML, starting from the optima found using CD. We find that the locations of the optima found using both methods differ substantially.

Figure 7 illustrates that the distances between the contrastive divergence optima and the corresponding ML optima are quite significant. The distances between the models found by ML training and CD training were found by flattening the weight matrix to a vector, concatenating the result with the bias vectors, and computing the Euclidean distance between the two vectors. Differences on the order of a few percent are observed in the limit of no noise. This suggests that the models learned using CD optimization and ML optimization can differ substantially. We see that these differences tend to increase as more hidden units are added to the model and that adding Bernoulli noise to the training data tends to cause the differences in the relative distances that arise from varying  $n_v$  to shrink.

Figure 8 shows that there are differences in the quality of the ML optima found as a function of the Bernoulli noise added to the training data, where quality is determined based on the value of  $O_{\text{ML}}$  at that point. The relative errors observed tend to be on the order of 0.1 percent for these examples, which is small but non-negligible given that differences in classification error on this order are significant in contemporary machine learning applications. The discrepancies in the values of  $O_{\text{ML}}$  follow similar trends to the data in Figure 7.

These results show, even for small examples, that significant differences exist between the locations and qualities

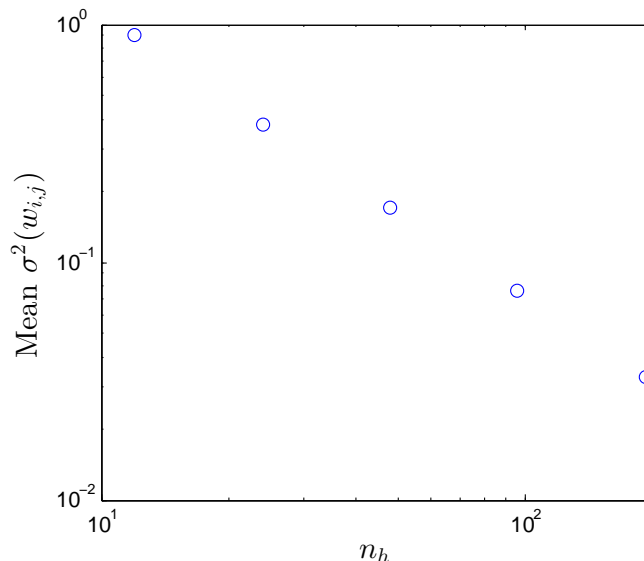


FIG. 6: Mean value of the variance of the weights for a RBM with  $n_v = 12$  and  $n_h = \{12, 24, 48, 96, 192\}$ . Each RBM was trained using 200,000 epochs on our synthetic data set with zero noise and learning rate 0.01 via CD-1. 100 different local optima were averaged for each point in the plot. The data follows a  $\sigma(w_{i,j})^2 \propto n_h^{-1.15}$  scaling.

of the CD and ML optima. Thus our quantum algorithms, which closely approximate ML training, are likely to lead to improved models over current state-of-the-art classical methods based on contrastive divergence if a reasonably small value of  $\kappa$  suffices. This point also is significant for classical machine learning approaches, wherein the use of more costly variants of contrastive divergence (such as CD- $k$  for  $k > 1$ ) may also lead to significant differences in the quality of models [7].

### E. Results for 3-layer dRBMs

Although the differences between contrastive divergence optimization and maximum-likelihood optimization were modest in the prior examples, we find that the differences between the quality of models learned in both cases can differ greatly, in particular when considering deep RBMs. In the following experiments, the maximum-likelihood training procedure is exactly the same as considered previously: we use BFGS optimization to maximize  $O_{\text{ML}}$  for a 3-layer deep BM. We then compute the value of the objective function and compare it to the results found by using greedy layerwise contrastive divergence training and present the data in Table II. We consider dRBMs containing three layers.

Unlike the single-layer RBM case, we do not perform CD-ML experiments. The reason for this is that the use of greedy training would potentially bias the ML results. Similarly, starting the contrastive divergence algorithm from a ML optima may obfuscate the effect of the greedy layer-wise training on the quality of the optima found. For this reason, we compare the mean values of  $O_{\text{ML}}$  found at the ML and CD optima corresponding to random initial models.

The first trend, as seen in Table II, is that for larger Boltzmann machines the quality of the optima found by contrastive divergence training is substantially worse than those found by optimizing the ML-objective function. In fact, differences on the order of 10% are observed for the models with 10 visible units. More data would be needed for the scaling of the relative differences to be meaningfully extracted. A notable exception occurs for the cases with  $n_{h1} = n_{h2} = 2$  for  $n_v \in \{8, 10\}$ . In such cases, the optima found by contrastive divergence tend to be better than those found by gradient ascent on  $O_{\text{ML}}$ . This is likely because the stochastic nature of contrastive divergence training gives the system the ability to escape from local optima that the ML training algorithm gets stuck in.

The most likely suspect for large discrepancies between the two training methods is the regularization term in  $O_{\text{ML}}$ . The log-likelihood of the Boltzmann machine producing the training vectors is increased by adding additional layers [3]. This does not imply that the ML objective function increases as more layers is added because of the presence of the regularization term. In fact, we find by comparing the 3-layer models that are greedily trained using contrastive divergence to those of the corresponding RBMs that the 3-layer models consistently have worse values of the ML objective function, despite having better log-likelihoods for the training data. This helps reconcile these results with previous work that has shown excellent classification accuracies for deep learning [3, 8]. Since the greedy

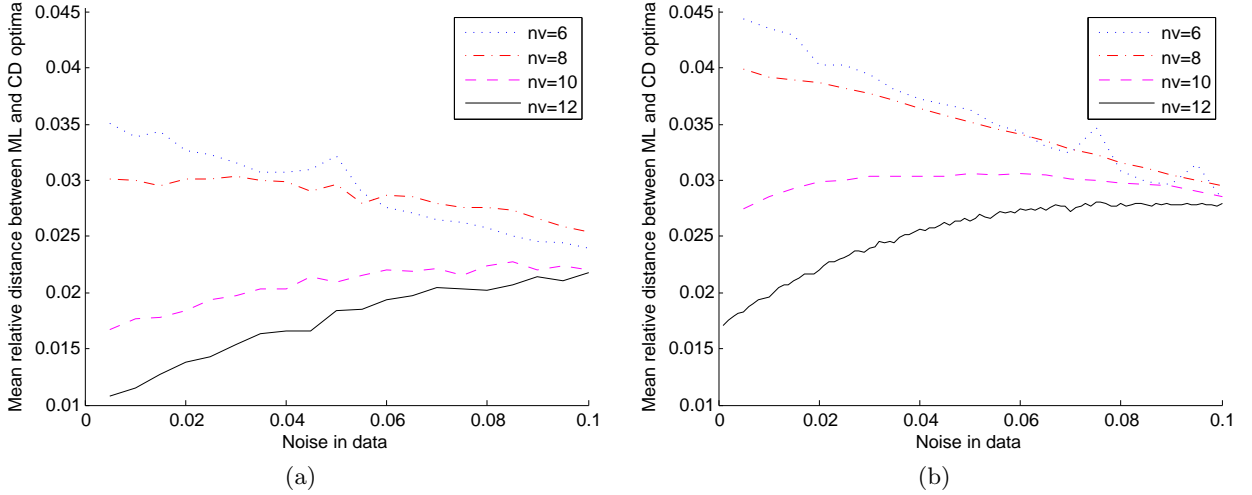


FIG. 7: Relative distances between the CD optima and ML optima for RBMs with  $n_v$  visible units and (a) 4 hidden units and (b) 6 hidden units.

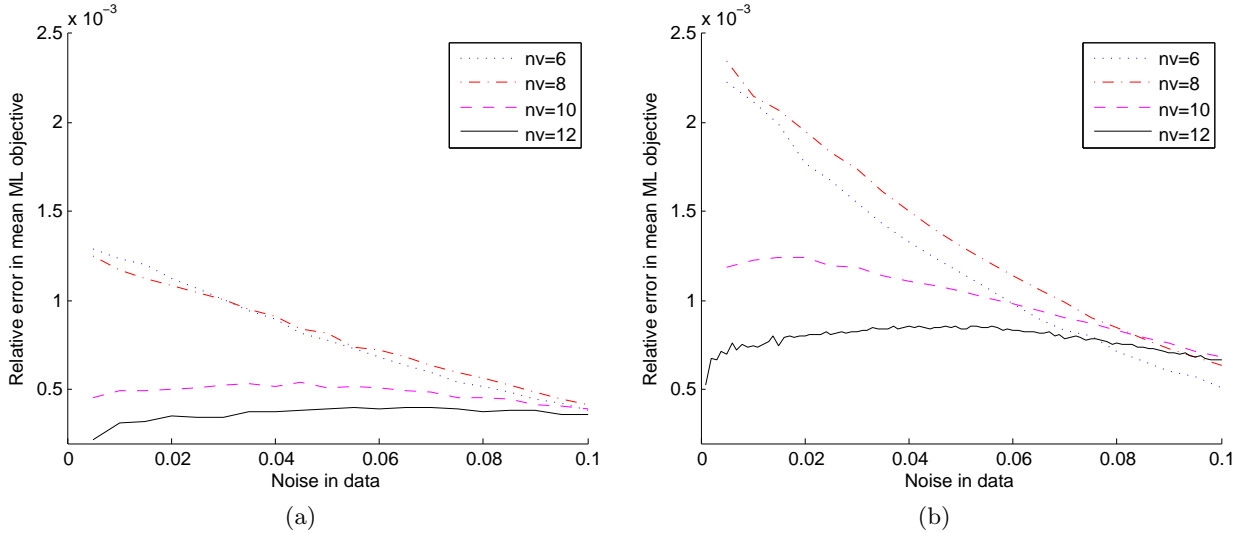


FIG. 8: Relative difference in the values of the ML objectives computed at the CD optima and the ML optima for RBMs with  $n_v$  visible units and (a) 4 hidden units and (b) 6 hidden units.

training process fails to optimize a global property, such as  $\lambda w^T w/2$ , these observations beg the question of whether greedy training properly protects against overfitting. This issue could lead to significant differences in classification accuracies for models trained using greedy contrastive divergence training and ML optimization.

### F. Training full Boltzmann machines under $O_{ML}$

The prior examples considered the performance of ML-based learning on single- and multi-layer restricted Boltzmann machines. Here we examine the quality of ML optima found when training a full Boltzmann machine with arbitrary connections between any two units. While classical training using contrastive divergence requires learning over a layered bipartite graph (dRBMs), our quantum algorithms do not need to compute the conditional distributions and can therefore efficiently train full Boltzmann machines given that the mean-field approximation to the Gibbs state has only polynomially small overlap with the true Gibbs state. The main question remaining is whether there are advantages to using a quantum computer to train such complete graphical models, and if such models exhibit superior performance over dRBMs.

$n_v$	$n_{h1}$	$n_{h2}$	CD	ML	% Improvement
6	2	2	-2.7623	-2.7125	1.80
6	4	4	-2.4585	-2.3541	4.25
6	6	6	-2.4180	-2.1968	9.15
8	2	2	-2.8503	-3.5125	-23.23
8	4	4	-2.8503	-2.6505	7.01
8	6	4	-2.7656	-2.4204	12.5
10	2	2	-3.8267	-4.0625	-6.16
10	4	4	-3.3329	-2.9537	11.38
10	6	4	-2.9997	-2.5978	13.40

TABLE II: Mean values of  $O_{\text{ML}}$  found via greedy training using contrastive divergence and BFGS optimization of  $O_{\text{ML}}$  for 3-layer deep Boltzmann machines. We also provide the percentage improvement in going from contrastive divergence training to ML training. Note that in several highly constrained cases ML does not typically find better optima than CD.

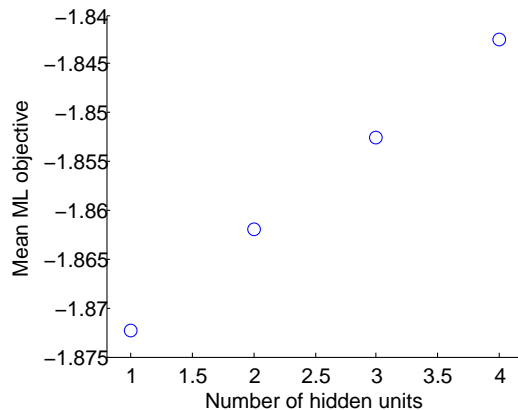


FIG. 9:  $O_{\text{ML}}$  for a fully connected Boltzmann machine with six visible units and one through four hidden units.

Figure 9 shows that the ML objective function found by training a full Boltzmann machine slowly improves the quality of the optima learned as the number of visible units increases. Although this increase is modest over the range of  $n_h$  considered, it is important to note that the value of the mean ML objective attained via BFGS optimization on a single-layer RBM with six visible and four hidden is approximately  $-2.33$ . Even the full Boltzmann machine with 7 units and 21 edges provided a much better model than an RBM with 10 units and 24 edges. Although this numerical example is quite small, it demonstrates the benefit of introducing full connectivity, namely intra-layer connections, to a Boltzmann machine and therefore suggests that our quantum learning algorithm may lead to better models than those that can be efficiently learned using existing methods.

An important limitation of this approach is that the mean-field approximation tends to be much worse for Ising models on the complete graph than it is for layered networks [34]. This means that the value of  $\kappa$  needed may also be larger for these systems. Although the results in [34] show acceptable performance in cases of small edge weight, further work is needed to investigate the trade off between model quality and training time for the quantum algorithm.

## VIII. CONCLUSION

Our work shows that quantum computing provides several advantages for deep learning. First, on a theoretical level, quantum computers appear well-suited for deep learning since many of the approximations used to make deep learning practical on classical computers are not needed for their quantum counterparts. Second, the quantum algorithms we propose continue to be efficient even in the presence of fully connected Boltzmann machines. This allows a much richer class of models to be efficiently trained than would otherwise be possible using existing classical methods. Finally, our algorithms show that quantum speedups over classical approaches are possible for Boltzmann machines that have many layers or utilize vast training sets. These results show that quantum computing has great promise as a platform for deep learning.

We also examine the discrepancies between the optima found by using contrastive divergence training and directly optimizing  $O_{\text{ML}}$ . Since our quantum algorithms closely approximate the latter approach, this serves as a good

surrogate for assessing the performance of our quantum algorithm in the absence of devices capable of implementing such algorithms. We find that while the locations of the corresponding optima can differ by a few percent for RBMs, the quality of the optima found differs on the order of a tenth of a percent. These differences are small, but meaningful given that state-of-the-art machine learning solutions vie for differences in classification accuracy on this order. When we compare the performance of both methods for training 3-layer restricted Boltzmann machines we observe differences in  $O_{ML}$  that are on the order of 10%. Our quantum algorithms therefore promise to yield much better models than those yielded by existing greedy layer-by-layer training algorithms. Finally, we examine the optima found for unrestricted Boltzmann machines and find that these models tend to lead to better models than RBMs with a comparable number of edges. These results suggest that there are quantitative advantages to training a Boltzmann machine using our quantum algorithms.

Looking forward, there are a number of extensions raised by this work. Firstly, it would be interesting to see the tradeoffs between improved success probability and complexity of preparing the initial state that arise from using approximations such as structured mean-field theory in place of mean-field theory. Such tradeoffs may be important to understand in cases that use small regularization constants. Secondly, we have not compared the performance of our algorithm and contrastive divergence via cross-validation because the cost of our numerical experiments grows exponentially with the number of label qubits. An examination of the performance of these algorithms in such scenarios would provide additional insight into whether the algorithms are equally likely to overfit the training data. Finally, although this work provides evidence that quantum computers may have value for accelerating training of deep Boltzmann machines, there may be even richer paradigms for performing machine learning in a quantum setting that do not have natural analogs in the classical machine learning literature. The discovery of such approaches may have profound implications for the future of artificial intelligence and related fields.

### Acknowledgments

We would like to thank Chris Burges for providing us with the code used for our contrastive divergence training experiments.

### Appendix A: Review of mean-field theory

The mean-field approximation is a variational approach that finds an uncorrelated distribution,  $Q(v, h)$ , that has minimal KL-divergence with the joint probability distribution  $P(v, h)$  given by the Gibbs distribution. The main benefit of using  $Q$  instead of  $P$  is that  $\langle v_i h_j \rangle_{\text{model}}$  and  $\log(Z)$  can be efficiently estimated using mean-field approximations [38]. A secondary benefit is that the mean-field state can be efficiently prepared using single-qubit rotations. More concretely, the mean-field approximation is a distribution such that

$$Q(v, h) = \left( \prod_i \mu_i^{v_i} (1 - \mu_i)^{1-v_i} \right) \left( \prod_j \nu_j^{h_j} (1 - \nu_j)^{1-h_j} \right), \quad (\text{A1})$$

where  $\mu_i$  and  $\nu_j$  are chosen to minimize  $\text{KL}(Q||P)$ . The parameters  $\mu_i$  and  $\nu_j$  are called mean-field parameters.

Using the properties of the Bernoulli distribution, it is easy to see that

$$\begin{aligned} \text{KL}(Q||P) &= \sum_{v, h} -Q(v, h) \ln(P(v, h)) + Q(v, h) \ln(Q(v, h)), \\ &= \sum_{v, h} Q(v, h) \left( \sum_i v_i b_i + \sum_j h_j d_j + \sum_{i, j} w_{i, j} v_i h_j + \ln Z \right) + Q(v, h) \ln(Q(v, h)) \\ &= \sum_i \mu_i b_i + \sum_j \nu_j d_j + \sum_{i, j} w_{i, j} \mu_i \nu_j + \ln(Z) \\ &\quad + \sum_i \mu_i \ln(\mu_i) + (1 - \mu_i) \ln(1 - \mu_i) + \sum_j \nu_j \ln(\nu_j) + (1 - \nu_j) \ln(1 - \nu_j). \end{aligned} \quad (\text{A2})$$

The optimal values of  $\mu_i$  and  $\nu_i$  can be found by differentiating this equation with respect to  $\mu_i$  and  $\nu_i$  and setting

the result equal to zero. The solution to this is

$$\begin{aligned}\mu_i &= \sigma(-b_i - \sum_j w_{i,j} \nu_j) \\ \nu_j &= \sigma(-d_j - \sum_i w_{i,j} \mu_i),\end{aligned}\tag{A3}$$

where  $\sigma(x) = 1/(1 + \exp(-x))$  is the sigmoid function. These equations can be implicitly solved by fixed point iteration, which involves initializing the  $\mu_i$  and  $\nu_j$  arbitrarily and iterate these equations until convergence is reached. Convergence is guaranteed provided that the norm of the Jacobian of the map is bounded above by 1. Solving the mean-field equations by fixed point iteration is analogous to Gibbs sampling with the difference being that here there are only a polynomial number of configurations to sample over and so the entire process is efficient. The generalization of this process to deep networks is straight forward and is discussed in [3].

Mean-field approximations to distributions such as  $P(v, h) = \delta_{v,x} \exp^{-E(x,h)} / Z_x$  can be computed using the exact same methodology. The only difference is that in such cases the visible units in the mean-field approximation is only taken over the hidden units. Such approximations are needed to compute the expectations over the data that are needed to estimate the derivatives of  $O_{\text{ML}}$  in our algorithms.

It is also easy to see from the above argument that among all product distributions,  $Q$  is the distribution that leads to the least error in the approximation to the log-partition function in (12). This is because

$$\log(Z_{\text{MF}}) = \log(Z) - \text{KL}(Q||P),\tag{A4}$$

and the mean-field parameters found by solving (A3) minimize the KL-divergence among all product distributions. It is also interesting to note that all such approximations are lower bounds for the log-partition function because  $\text{KL}(Q||P) \geq 0$ .

Experimentally, mean-field approximations can estimate the log-partition function within less than 1% error [39] depending on the weight distribution and the geometry of the graph used. We further show in Section VII C that the mean-field approximation to the partition function is sufficiently accurate for small restricted Boltzmann machines. Structured mean-field approximation methods [35], TAP [36] or AIS [8, 37] can be used to reduce such errors if needed, albeit at a higher classical computational cost.

These results also suggest the following result, which shows that the success probability of our state preparation method approaches 1 in the limit where the strengths of the correlations in the model vanish.

**Corollary 2.** *The success probability in Lemma 2 approaches 1 as  $\max_{i,j} |w_{ij}| \rightarrow 0$ .*

*Proof.* The energy is a continuous function of  $w$  and therefore  $e^{-E(v,h)} / Z$  is also a continuous function of  $w$ . Therefore,  $\lim_{w \rightarrow 0} P(v, h) = e^{-\sum_i b_i v_i - \sum_j b_j h_j} / \sum_{v,h} e^{-\sum_i b_i v_i - \sum_j b_j h_j}$ . Under such circumstances,  $P(v, h)$  factorizes and so there exist  $\tilde{\mu}_i$  and  $\tilde{\nu}_j$  such that

$$\lim_{w \rightarrow 0} P(v, h) = \left( \prod_i \tilde{\mu}_i^{v_i} (1 - \tilde{\mu}_i)^{1-v_i} \right) \left( \prod_j \tilde{\nu}_j^{h_j} (1 - \tilde{\nu}_j)^{1-h_j} \right).\tag{A5}$$

Hence it follows from (A1) that there exists a mean-field solution such that  $\text{KL}(Q||\lim_{w \rightarrow 0} P) = 0$ . Since the solution to (A3) is unique when  $w_{i,j} = 0$  it follows that the mean-field solution found must be the global optima and hence there  $\text{KL}(Q||P)$  approaches 0 as  $\max_{i,j} |w_{i,j}| \rightarrow 0$ . Therefore (A4) implies that  $Z_{\text{MF}} \rightarrow Z_{x,\text{MF}}$  in the limit. Hence as  $\max_{i,j} |w_{i,j}| \rightarrow 0$  we can take  $\kappa = 1$  and  $Z/Z_{\text{MF}} = 1$ . Therefore the success probability approaches 1 if the optimal value of  $\kappa$  is chosen. The same argument also applies for  $Z_x/Z_{x,\text{MF}}$ .  $\square$

## Appendix B: Review of contrastive divergence training

The idea behind contrastive divergence is straightforward. The model average in (4) can be computed by sampling from the Gibbs distribution  $P$ . This process is not tractable classically, so contrastive divergence samples from an approximation to the Gibbs distribution found by applying a finite number of rounds of Gibbs sampling. The resultant samples drawn from the distribution are then, ideally, drawn from a distribution that is close to the true Gibbs distribution  $P$ .

Gibbs sampling proceeds as follows. First the visible units are set to a training vector. Then the hidden units are set to 1 with probability  $P(h_j = 1|v) = \sigma(-d_j - \sum_i w_{i,j} v_i)$ . Once the hidden units are set, the visible units are reset

to 1 with probability  $P(v_i = 1|h) = \sigma(-b_i - \sum_j w_{i,j}h_j)$ . This process can then be repeated using the newly generated training vector in place of the original  $v$ . As the number of rounds of Gibbs sampling increases, the distribution over resultant samples approaches that of the true Gibbs distribution.

The simplest contrastive divergence algorithm, CD-1, works by using only one round of Gibbs sampling to reset the visible units. The probability that each of the hidden units is 1 is then computed using  $P(h_j = 1|v) = \sigma(-d_j - \sum_i w_{i,j}v_i)$ . These probabilities are stored and the process of Gibbs sampling and probability computation is repeated for each training vector. The probabilities necessary for the model average are then set, for each  $w_{i,j}$ , to be the average of all the probabilities  $\Pr(v_i = 1, h_j = 1)$  computed in the prior samples. Closer approximations to the Gibbs distribution can be found by using more steps of Gibbs sampling [7, 11, 33]. For example, CD-10 uses ten steps of Gibbs sampling rather than one and tends to give much better approximations to the true gradient of the objective function.

Contrastive divergence earns its name because it does not try to approximate the gradients of the ML-objective function; rather, CD- $n$  approximately optimizes the difference between the average log-likelihood after zero and  $n$  rounds of Gibbs sampling:  $\text{KL}(p_0||p_\infty) - \text{KL}(p_n||p_\infty)$  [5]. Also as  $n \rightarrow \infty$  the contrastive divergence objective becomes the average log-likelihood, which is  $O_{\text{ML}}$  in the absence of regularization. This means that asymptotically CD- $n$  approximates the correct derivatives. Although contrastive divergence approximates the gradient of the contrastive divergence objective function, the gradients yielded by the algorithm are not precisely the gradients of any objective function [9]. Thus the analogy of contrastive divergence optimizing an objective function that is close to  $O_{\text{ML}}$  is inexact.

Although it is efficient, there are several drawbacks to contrastive divergence training. The main drawback of CD is that it does not permit interactions between hidden and visible units. This restricts the allowable class of graphical models. Additionally, the training process can take hours to days [7]. Finally, the method does not directly apply to training deep networks. In order to train deep restricted Boltzmann machines, layer-wise training is typically employed, which breaks the undirected structure of the network and potentially leads to sub-optimal models. Our work shows that quantum computing provides the means to circumvent such restrictions.

- 
- [1] Geoffrey Hinton, Simon Osindero, and Yee-Whye Teh. A fast learning algorithm for deep belief nets. *Neural computation*, 18(7):1527–1554, 2006.
  - [2] Ronan Collobert and Jason Weston. A unified architecture for natural language processing: Deep neural networks with multitask learning. In *Proceedings of the 25th international conference on Machine learning*, pages 160–167. ACM, 2008.
  - [3] Yoshua Bengio. Learning deep architectures for ai. *Foundations and trends® in Machine Learning*, 2(1):1–127, 2009.
  - [4] Yann LeCun, Koray Kavukcuoglu, and Clément Farabet. Convolutional networks and applications in vision. In *Circuits and Systems (ISCAS), Proceedings of 2010 IEEE International Symposium on*, pages 253–256. IEEE, 2010.
  - [5] Geoffrey E Hinton. Training products of experts by minimizing contrastive divergence. *Neural computation*, 14(8):1771–1800, 2002.
  - [6] Ruslan Salakhutdinov, Andriy Mnih, and Geoffrey Hinton. Restricted boltzmann machines for collaborative filtering. In *Proceedings of the 24th international conference on Machine learning*, pages 791–798. ACM, 2007.
  - [7] Tijmen Tieleman. Training restricted boltzmann machines using approximations to the likelihood gradient. In *Proceedings of the 25th international conference on Machine learning*, pages 1064–1071. ACM, 2008.
  - [8] Ruslan Salakhutdinov and Geoffrey E Hinton. Deep boltzmann machines. In *International Conference on Artificial Intelligence and Statistics*, pages 448–455, 2009.
  - [9] Ilya Sutskever and Tijmen Tieleman. On the convergence properties of contrastive divergence. In *International Conference on Artificial Intelligence and Statistics*, pages 789–795, 2010.
  - [10] Tijmen Tieleman and Geoffrey Hinton. Using fast weights to improve persistent contrastive divergence. In *Proceedings of the 26th Annual International Conference on Machine Learning*, pages 1033–1040. ACM, 2009.
  - [11] Yoshua Bengio and Olivier Delalleau. Justifying and generalizing contrastive divergence. *Neural Computation*, 21(6):1601–1621, 2009.
  - [12] Asja Fischer and Christian Igel. Bounding the bias of contrastive divergence learning. *Neural computation*, 23(3):664–673, 2011.
  - [13] Nathan Wiebe, Daniel Braun, and Seth Lloyd. Quantum algorithm for data fitting. *Physical review letters*, 109(5):050505, 2012.
  - [14] Guoming Wang. Quantum algorithms for curve fitting. *arXiv preprint arXiv:1402.0660*, 2014.
  - [15] Esma Aïmeur, Gilles Brassard, and Sébastien Gambs. Machine learning in a quantum world. In *Advances in Artificial Intelligence*, pages 431–442. Springer, 2006.
  - [16] Esma Aïmeur, Gilles Brassard, and Sébastien Gambs. Quantum clustering algorithms. In *Proceedings of the 24th international conference on machine learning*, pages 1–8. ACM, 2007.
  - [17] Seth Lloyd, Masoud Mohseni, and Patrick Rebentrost. Quantum algorithms for supervised and unsupervised machine learning. *arXiv preprint arXiv:1307.0411*, 2013.

- [18] Patrick Rebentrost, Masoud Mohseni, and Seth Lloyd. Quantum support vector machine for big feature and big data classification. *arXiv preprint arXiv:1307.0471*, 2013.
- [19] Nathan Wiebe, Ashish Kapoor, and Krysta Svore. Quantum nearest-neighbor algorithms for machine learning. *QIC*, 15:318–358, 2015.
- [20] Guang Hao Low, Theodore J Yoder, and Isaac L Chuang. Quantum inference on bayesian networks. *arXiv preprint arXiv:1402.7359*, 2014.
- [21] Hartmut Neven, Vasil S Denchev, Geordie Rose, and William G Macready. Training a large scale classifier with the quantum adiabatic algorithm. *arXiv preprint arXiv:0912.0779*, 2009.
- [22] Michael A Nielsen and Isaac L Chuang. *Quantum computation and quantum information*. Cambridge university press, 2010.
- [23] Vadym Kliuchnikov, Dmitri Maslov, and Michele Mosca. Fast and efficient exact synthesis of single-qubit unitaries generated by clifford and t gates. *Quantum Information & Computation*, 13(7-8):607–630, 2013.
- [24] Neil J Ross and Peter Selinger. Optimal ancilla-free clifford+ t approximation of z-rotations. *arXiv preprint arXiv:1403.2975*, 2014.
- [25] Alex Bocharov, Martin Roetteler, and Krysta M Svore. Efficient synthesis of universal repeat-until-success circuits. *arXiv preprint arXiv:1404.5320*, 2014.
- [26] Maris Ozols, Martin Roetteler, and Jérémie Roland. Quantum rejection sampling. *ACM Transactions on Computation Theory (TOCT)*, 5(3):11, 2013.
- [27] David Poulin and Pawel Wocjan. Sampling from the thermal quantum gibbs state and evaluating partition functions with a quantum computer. *Physical review letters*, 103(22):220502, 2009.
- [28] Gilles Brassard, Peter Hoyer, Michele Mosca, and Alain Tapp. Quantum amplitude amplification and estimation. *arXiv preprint quant-ph/0005055*, 2000.
- [29] Lov K Grover. A fast quantum mechanical algorithm for database search. In *Proceedings of the twenty-eighth annual ACM symposium on Theory of computing*, pages 212–219. ACM, 1996.
- [30] Nathan Wiebe and Martin Roetteler. Quantum arithmetic and numerical analysis using repeat-until-success circuits. *arXiv preprint arXiv:1406.2040*, 2014.
- [31] Vittorio Giovannetti, Seth Lloyd, and Lorenzo Maccone. Quantum random access memory. *Physical review letters*, 100(16):160501, 2008.
- [32] Pinar Donmez, Krysta M Svore, and Christopher JC Burges. On the local optimality of lambdarank. In *Proceedings of the 32nd international ACM SIGIR conference on Research and development in information retrieval*, pages 460–467. ACM, 2009.
- [33] Miguel A Carreira-Perpinan and Geoffrey E Hinton. On contrastive divergence learning. In *Proceedings of the tenth international workshop on artificial intelligence and statistics*, pages 33–40. Citeseer, 2005.
- [34] Martin J Wainwright, Tommi S Jaakkola, and Alan S Willsky. A new class of upper bounds on the log partition function. *Information Theory, IEEE Transactions on*, 51(7):2313–2335, 2005.
- [35] Eric P Xing, Michael I Jordan, and Stuart Russell. A generalized mean field algorithm for variational inference in exponential families. In *Proceedings of the Nineteenth conference on Uncertainty in Artificial Intelligence*, pages 583–591. Morgan Kaufmann Publishers Inc., 2002.
- [36] Manfred Opper and Ole Winther. Tractable approximations for probabilistic models: The adaptive thouless-anderson-palmer mean field approach. *Physical Review Letters*, 86(17):3695, 2001.
- [37] Ruslan Salakhutdinov and Iain Murray. On the quantitative analysis of deep belief networks. In *Proceedings of the 25th international conference on Machine learning*, pages 872–879. ACM, 2008.
- [38] Michael I Jordan, Zoubin Ghahramani, Tommi S Jaakkola, and Lawrence K Saul. An introduction to variational methods for graphical models. *Machine learning*, 37(2):183–233, 1999.
- [39] Martijn AR Leisink and Hilbert J Kappen. A tighter bound for graphical models. In *NIPS*, volume 13, pages 266–272, 2000.
- [40] Max Welling and Geoffrey E Hinton. A new learning algorithm for mean field boltzmann machines. In *Artificial Neural Networks ICANN 2002*, pages 351–357. Springer, 2002.